PLC BASED SOLAR TRACKING SYSTEM

Design and Programming of Linear Motors in an Autonomous Solar Tracking System

HAMK
HÄMEEN AMMATTIKORKEAKOULU
HÄME UNIVERSITY OF APPLIED SCIENCES

Bachelor's thesis

Electrical Engineering and Automation

Spring 2021, Valkeakoski

Eron Shuku
Nedim Ates Karadadas

Electrical Engineering and Automation
Valkeakoski

Authors	Eron Shuku; Nedim Ates Karadadas	**Year** 2021
Subject	PLC Based Solar Tracking System	
Supervisor(s)	Katariina Penttilä	

ABSTRACT

This thesis was commissioned by the Electrical Engineering and Automation degree programme at the Häme University of Applied Sciences (HAMK), with Katariina Penttilä as the thesis supervisor. The target of this project was to establish a solar tracking system with programmable logic controller as its controlling unit. More specifically this project concerned the programming of the linear motors that were used to move the solar panel into the desired angle. Furthermore, a comparison was drawn between traditional static solar panels and various tracking systems. This was done by examining other peer reviewed research into the effectiveness of such systems in different environmental conditions, as real-life testing of this particular system was difficult to prepare during the Covid-19 pandemic.

The programming of the system was done with a Siemens Programmable Logic Controller, specifically the S7-1200 series, through TIA Portal v15.1. Hardware wise, it had two linear motors, which had a feedback system and through retraction and extension, move a panel at the optimal angle. To accomplish this, a sun position calculating algorithm, developed by the National Renewable Energy Laboratory in the United States, was used, as well as its adaptation by Siemens. The algorithm provided the angle at which the panel would be positioned and moved the motors there automatically. In addition, there was a manual mode, which allowed the user to adjust the panel angle at the preferred position. The tracking in this system, was both single, and dual axis. In the single axis mode, the Y-axis motor was static, whilst the X-axis motor derived its data from Siemens' PHI angle calculator function block. This provided an angle in which the panel needs to be repositioned for optimal tracking. Dual tracking utilized the zenith and sunset and sunrise times for motor tracking.

Dual axis tracking is a difficult and costly method to implement. Using sunrise and sunset times to facilitate dual axis tracking is an atypical and unproven method, and warrants more research before implementation. On the other hand, the single axis feature of the system is an accurate and established approach, with promising earlier results. When in range, the system has a tracking accuracy of ±1°. Data analysis from research shows that even a single axis three-position system can increase efficiency and make solar tracking a worthwhile endeavour.

Keywords Automated tracking, Linear motors, PLC, Solar tracking, Solar panels.

Pages 45 pages

CONTENTS

LIST OF FIGURES

LIST OF TABLES

1 INTRODUCTION

Consumption of solar power in Finland started by measuring at 17 TJ in 1988. Since then, there has been a significant increase in usage of solar energy, reaching 733 TJ in 2019. (Official Statistics of Finland, 2019)

Despite this upsurge, total production of solar power in Finland from photovoltaic (PV) systems remains low, 178 GWh or only 0.2% of all electricity sources (Official Statistics of Finland, 2019). One key factor explaining these statistics, is the lack of incentives provided by the Finnish government. This is in contrast with the policies of the German government where feed in tariffs (FIT) have been introduced for solar and wind power. FIT is a fixed price incentive at which individual manufacturers can sell electricity and are generally given priority access to the grid (Appunn & Wehrmann, 2019). Currently, in Finland it is not feasible to invest into a PV system compared to other energy sources. Plants commissioned in 2013 receive 104–151 EUR/MWh, whilst similar projects in Germany reach 290 EUR/MWh. If these were to be used in Finland, a 60kW PV system which would normally have a payback period of well over 50 years, would see that decline to just eight years. (Hakkarainen, Tsupari, Hakkarainen, & Ikäheimo, 2015).
The EU and Finland are setting new carbon emission and renewable energy targets, this makes research for efficiency increase of existing technologies imperative (European Commission, 2020).

With irradiation levels in Finland being comparable to Germany (Hakkarainen, Tsupari, Hakkarainen, & Ikäheimo, 2015) this project examined the usage of a sun tracking solar panel, its serviceability, and feasibility in the given environment in contrast to fixed mount systems, the latter having often been the point of research.

1.1 Outline of Thesis

This thesis is divided into four main chapters. Chapter one details the background and targets of the thesis, discussing the issue at hand in detail.

Chapter two lays out the theoretical background of the project, detailing the methods utilized in order to achieve the end goal. This includes solar positioning, the National Renewable Energy Laboratory's Solar Position Algorithm and its adaptation in the Siemens software, the geographical and astronomical parameters needed, as well as the software and hardware configuration.

Chapter three describes the implementation of Siemens' adaptation of the solar tracking algorithm, in addition to the architectural structure of the programming configured.

Chapter four discusses the results obtained from limited testing of the system, and analyses existing research into solar tracking systems.

1.2 Background and Project Targets

The project has been commissioned by the Häme University of Applied Sciences (HAMK). A version of this tracking solution has been implemented previously at HAMK, which used Arduino microcontrollers in combination with light sensors to achieve automatic solar tracking. The version described in the thesis implements a Siemens PLC based solution, relying on a tracking algorithm to locate the position of the sun; more specifically, the configuration of the linear motors used to move the solar panel.

The target of this project is to research the possibility of building an algorithm-based sun tracking solar panel system, compact enough to study its efficiency and value against a static non-tracking solar panel, in the HAMK research environment in the future. These results can be the basis of further research and teaching possibilities. In addition, this paper investigates previous works and their results, to gain a better understanding of the feasibility of such systems.

1.3 Division of Labour

Whilst most of the work was done jointly, table 1 shows a simplified labour distribution of the thesis, addressing the written and empirical parts.

Table 1. Division of Labour

Written Part (Sub-Chapters)		
Eron	**Joint**	**Ates**
Spa Function	Introduction	PLC System
Solar Positioning	Conclusion	PLC Program
Solar Tracking with NREL SPA		Hardware Configuration
Results and Analysis		
Empirical Part		
Eron	**Joint**	**Ates**
Data Gathering	PLC cabinet Hardware Setup	Communication with Siemens Representatives
Motor Movement Programming		HMI Programming and Setup

2 THEORY

This chapter concerns the theoretical background on the essential theory used in the course of this project. When analysing solar tracking it is necessary to recognise the movement and positioning of the sun and how this relates to the tracking algorithm, with all real-life challenges such as the range of the gear in use.

2.1 Solar Positioning

When tackling solar positioning, there are a number of parameters, such as the azimuth, zenith, and elevation angle of the sun, that need to be taken into account. Fig.1 shows the movement of the sun in the sky from a topocentric point of view, marking all the necessary angles.

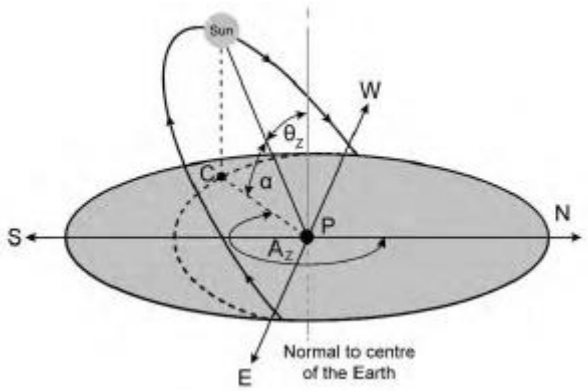

Figure 1. Sun vector components in a diurnal circle course of the sun (Prinsloo & Dobson, 2015)

Θ_Z – represents the zenith angle, which is the angle between the topocentric zenith and the sun vector (ε).
A_Z – represents the azimuth angle, which can be defined as the angle between the vertical of the sun to the vertical of the true north.
A- is the angle between the plane and the sun vector (ε), also known as the elevation angle.
P – is the observer point of view.
C – is the point where the sun vertical meets the plane.

The sun vector is comprised of the azimuth and the elevation angle ε (A_Z, α). This is the true position of the sun as seen from an observer on the surface of the earth. From fig. 1 it can be determined that the zenith is normal to the horizontal plane, and is a sum of the elevation angle and the solar zenith as shown in the following formula:

$$Zenith\ (90°) = \alpha + \Theta_Z \qquad (1)$$

(Prinsloo & Dobson, 2015)

2.2 **Solar Tracking with NREL SPA**

A solar tracking system refers to a system which is able to track the movement of the sun throughout the day for maximum energy efficiency and have it at a perpendicular angle to the plane of the solar panel. This can be achieved in two distinct approaches, closed loop and open loop controllers. Closed loop systems (Feedback controllers) typically utilize light sensors to determine the current sun position. However, issues arise when the system is met with low insolation conditions such as cloudy days, or at dawn; the trackers get confused as the sensors are not receiving reliable data. On the other hand, open-loop controllers do not employ the use of sensors, instead relying on a predetermined set of data on the sun's position to govern the movement of the panel. (Reca-Cardeña & López-Luque, 2018)

The most commonly used algorithm here is the National Renewable Energy Laboratory (NREL)'s solar position algorithm (SPA); which was developed in May 2003 and revised in January 2008. This is what Siemens utilizes to create their own sun tracking tools.

2.2.1 Operating Principle and Siemens Application

Ibrahim Reda and Afshin Andreas, 2008, in their "Solar Position Algorithm for Solar Radiation Applications" report define a process for a solar position algorithm with which they are able to determine the zenith and azimuth angle of the sun with a ±0.0003° error range, from the year -2000 to 6000.

Siemens SIMATIC S7-1200 is one of the PLC lines which provides solar tracking for the end user. Fig. 2 shows the SIMATIC S7-1200 solar tracker control architecture for dual axis tracking. As it can be seen in the figure the zenith and azimuth drive the motor movement in the dual axis system.

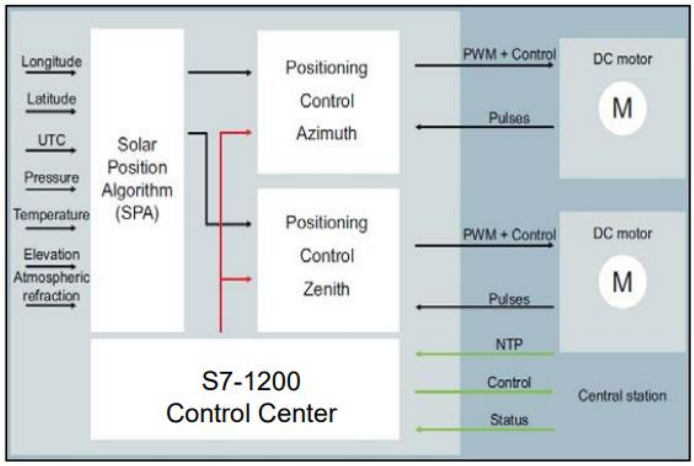

Figure 2. SIMATIC S7-1200 Solar Tracker Control Architecture (Tang, 2014)

This process is conducted through the solar tracking and the calculation of the alignment for single axis tracking libraries, depending on whether the system is single or dual axis.

The Siemens SPA (Solar Position Algorithm) calculates the azimuth and zenith. Fig. 3 shows the function block in the software and Table 2 contains its inputs, outputs, and respective properties. (Siemens AG, 2020)

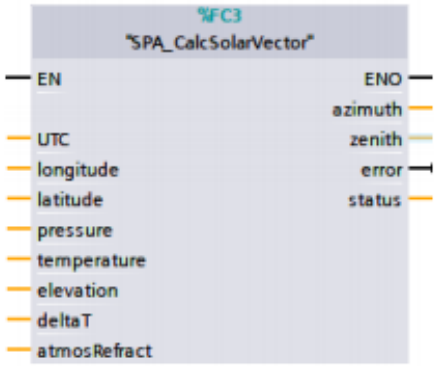

Figure 3. SPA function block as seen in TIAPortal (Siemens AG, 2020)

Table 2. Properties of parameters (Siemens AG, 2020)

Variable	Data Type	I/O Type	Unit	Project Value	Notes
UTC	DTL	Input	-	Current time and date	Universal Time
Longitude	LREAL	Input	Degree [°]		Longitude of the point
Latitude	LREAL	Input	Degree [°]		Latitude of the point
Pressure	LREAL	Input	Millibar [mbar]	1010	Ambient pressure
Temperature	LREAL	Input	Celsius Degree [°C]	7	Ambient Temperature
Elevation	LREAL	Input	Meter [m]	88	Elevation
Delta_T	LREAL	Input	Second [s]	See Chapter 2.2.3	Difference between earth rotation and terrestrial time
Atmos_Refract	LREAL	Input	Degree [°]	0.5567	Sunrise and sunset refraction
Azimuth	LREAL	Output	Degree [°]	-	Topocentric Azimuth
Zenith	LREAL	Output	Degree [°]	-	Topocentric Zenith
Error	Bool	Output	-	-	Error flag
Status	Word	Output	-	-	Error message

The position of the sun can be determined by the zenith and azimuth and used for dual axis tracking; however, if the tracking system is single axis, then the calculation of alignment for single axis tracking library must be used. The function block of this library, shown below in Fig. 4, converts the azimuth and zenith angle into one PHI (ϕ) angle.

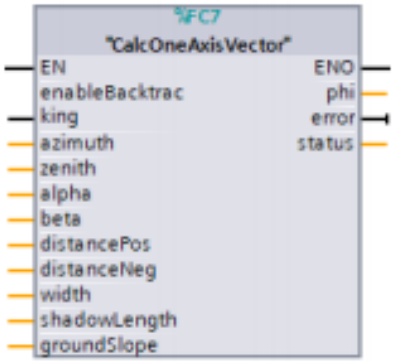

Figure 4. Single axis vector function block (Siemens AG, 2020)

Table 2 also shows the parameters of the "CalcOneAxisVector" function block.

Table 3. Properties of parameters for single axis tracking

Variable	Data Type	I/O Type	Unit	Project Value	Notes
Enable Backtracking	Bool	Input	-	0	Enables backtracking feature
Azimuth	LREAL	Input	Degree [°]	*Data*	Taken from the previous function block
Zenith	LREAL	Input	Degree [°]	*Data*	Taken from the previous function block
Alpha	LREAL	Input	Degree [°]	180	Rotation of the panel around the azimuth
Beta	LREAL	Input	Degree [°]	30	Rotation of the module around zenith
DistancePos	LREAL	Input	Meter [m]	-	Distance between two trackers in the morning
DistanceNeg	LREAL	Input	Meter [m]	-	Distance between two trackers in the afternoon
Width	LREAL	Input	Meter [m]	-	Width of heliostat
ShadowLengh	LREAL	Input	Meter [m]	-	Length of allowed shadow
GroundSlope	LREAL	Input	Degree [°]	-	Slope of ground
Phi	LREAL	Output	Degree [°]	-	Most effective angle of tracking for the panel
Error	Bool	Output	-	-	Error flag
Status	Word	Output	-	-	Error message

(Siemens AG, 2020)

Single axis tracking means that one axis is fixed and cannot move. Apart from the zenith and azimuth, the rotation and slope of the tracker; Alpha and Beta respectively, need to be fed to the algorithm. Fig. 5 demonstrates this. (Siemens AG, 2020)

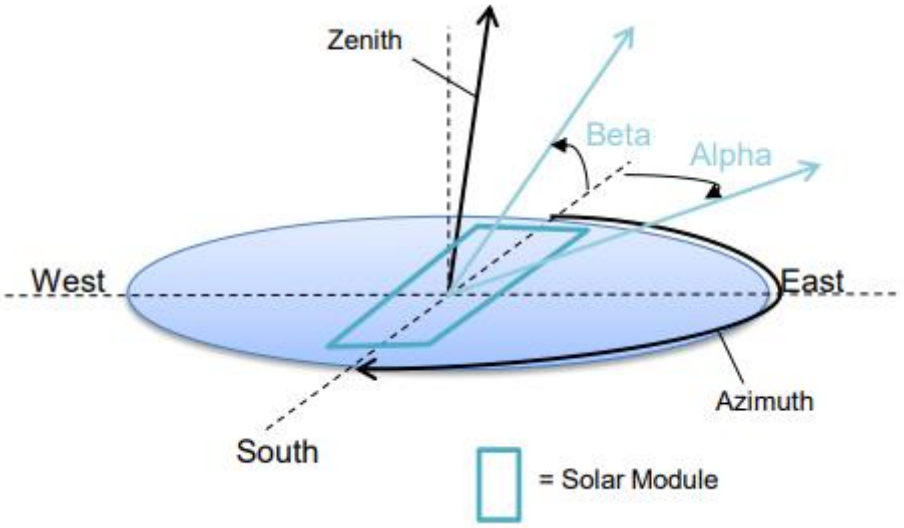

Figure 5. Representation of the azimuth, zenith, slope, and rotation angles in the horizontal plane. (Siemens AG, 2020)

Fig. 5 shows that when the panel faces south, Alpha is 180°. The system portrayed in this thesis when using single tracking, the slope was fixed at 30° as shown in Fig. 6

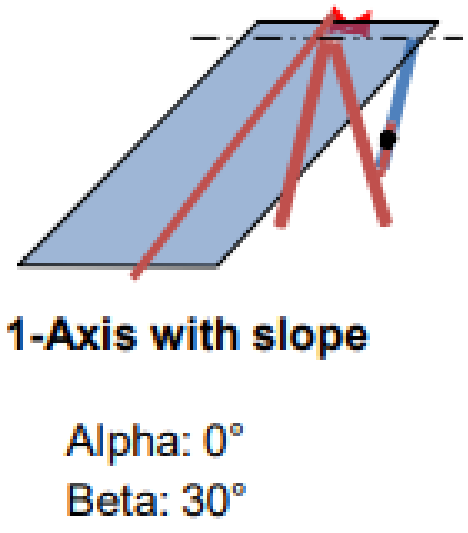

Figure 6. Single axis tracking system with a fixed slope at 30° (Siemens AG, 2020)

2.2.2 Accuracy of Siemens Solar Position Algorithm

In his journal article “Effects of parameters on NREL Solar Position Algorithm (SPA) and SIMATIC S7-1200 SPA_Calc_SunVector library accuracy” (Tang, 2014) compares the accuracy of a Siemens SIMATIC S7-1200 to a “Sun Vector Calculator” PC software utilizing the NREL-SPA algorithm. Fig. 7 shows the azimuth and zenith accuracy plotted against a time graph to display precision fluctuations throughout the day.

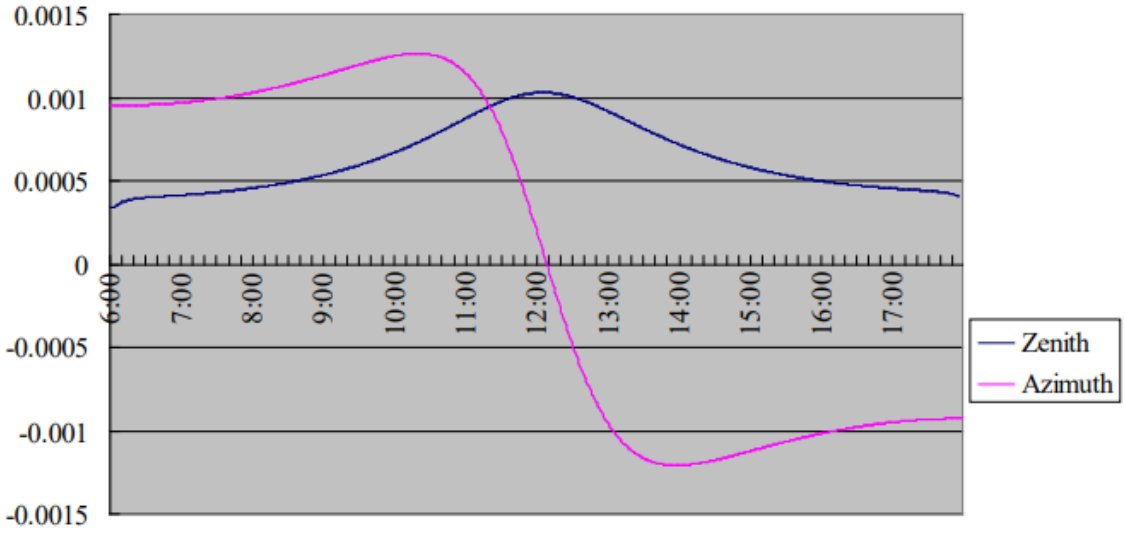

Figure 7. Accuracy of zenith and azimuth calculations throughout the day. (Tang, 2014)

The acceptable error rate here when taking into account mechanical and gear precision is ±0.05°. When held to this standard, Siemens SPA can be considered accurate. Based on Fig. 7 the following assumptions can be made. (Tang, 2014)

1. The algorithm is most accurate at three stages; sunrise, sunset, and local sun transit or moment when the sun is at the highest point in the sky. (Chmielewski, 2017).
2. Azimuth is least accurate one hour before and one hour after sun transit.
3. On the other hand, the zenith is least accurate during local sun transit. (Tang, 2014)

Based on this and other tests and comparisons made in Tang’s paper, Table 4 of parameter significance could be made.

Table 4. Significance of SPA Parameters. (Tang, 2014)

Parameters	Significance Level		
	Significant	Insignificant	No Effect
Local Time	X		
Delta_T		X	
Time Zone	X		
Longitude	X		
Latitude	X		
Elevation		X	
Pressure		X	
Temperature		X	
Slope			X

2.2.3 Delta_T Calculations

Delta_T refers to difference between the earth rotation time and terrestrial time. For the time period 2005 – 2050 it can be calculated using the following equation:

$$\Delta T = 62.92 + 0.32217 * t + 0.005589 * t^2 \quad (2)$$

(Morrison & Stephenson, 2004)

where: $t = y - 2000$ (3)

(Morrison & Stephenson, 2004)

ΔT is Delta_T and y is the year which is defined as follows

$$y = year + \frac{(month - 0.5)}{12} \quad (4)$$

(Morrison & Stephenson, 2004)

When applying this equation to Table 5, the Delta_T between the years 2005 – 2023 in the month of April could be calculated.

Table 5. Delta_T for 2005 – 2023 in the month of April (Morrison & Stephenson, 2004)

Constants for 2005 – 2050			t	Year	Year (Y)	Delta_T
62.92	0.32217	0.005589	5.291667	2005	2005.292	64.78
62.92	0.32217	0.005589	6.291667	2006	2006.292	65.17
62.92	0.32217	0.005589	7.291667	2007	2007.292	65.57
62.92	0.32217	0.005589	8.291667	2008	2008.292	65.98
62.92	0.32217	0.005589	9.291667	2009	2009.292	66.40
62.92	0.32217	0.005589	10.29167	2010	2010.292	66.83
62.92	0.32217	0.005589	11.29167	2011	2011.292	67.27
62.92	0.32217	0.005589	12.29167	2012	2012.292	67.72
62.92	0.32217	0.005589	13.29167	2013	2013.292	68.19
62.92	0.32217	0.005589	14.29167	2014	2014.292	68.67
62.92	0.32217	0.005589	15.29167	2015	2015.292	69.15
62.92	0.32217	0.005589	16.29167	2016	2016.292	69.65
62.92	0.32217	0.005589	17.29167	2017	2017.292	70.16
62.92	0.32217	0.005589	18.29167	2018	2018.292	70.68
62.92	0.32217	0.005589	19.29167	2019	2019.292	71.22
62.92	0.32217	0.005589	20.29167	2020	2020.292	71.76
62.92	0.32217	0.005589	21.29167	2021	2021.292	72.31
62.92	0.32217	0.005589	22.29167	2022	2022.292	72.88
62.92	0.32217	0.005589	23.29167	2023	2023.292	73.46

A similar table collecting monthly data for the period of January 2020 – July 2021 is shown in Table 6.

Table 6. Delta_T for Jan 2020 – July 2021 (Morrison & Stephenson, 2004)

New t	Year (Y)	Month	Delta_T
20.04167	2020.042	Jan	71.62175
20.125	2020.125	Feb	71.6673
20.20833	2020.208	Mar	71.71294
20.29167	2020.292	Apr	71.75865
20.375	2020.375	May	71.80443
20.45833	2020.458	Jun	71.8503
20.54167	2020.542	Jul	71.89624
20.625	2020.625	Aug	71.94226
20.70833	2020.708	Sep	71.98836
20.79167	2020.792	Oct	72.03454
20.875	2020.875	Nov	72.08079
20.95833	2020.958	Dec	72.12712
21.04167	2021.042	Jan	72.17353
21.125	2021.125	Feb	72.22002
21.20833	2021.208	Mar	72.26658
21.29167	2021.292	Apr	72.31323
21.375	2021.375	May	72.35995
21.45833	2021.458	Jun	72.40674
21.54167	2021.542	Jul	72.45362

2.3 **PLC System**

A programmable logic controller (PLC) is a specifically designed CPU that can control variety of automation applications. CPU and the programming tools allow users to design autonomous industrial processes and solve automation problems. Based on this specific application and its user-friendly programming tool and troubleshooting solutions, Siemens' PLC hardware and software were found to be the right fit for the automatic solar tracking application in this project. (Siemens, 2016)

2.3.1 Operating Principle

A CPU consists of a microprocessor, an integrated power supply, input and output circuits, built-in PROFINET, high-speed motion control I/O, and on-board analog inputs in a compact housing to create a powerful controller. As the user downloads the logic program, the CPU have the logic required to monitor and control the devices in your application. The CPU processes the inputs and changes the outputs according to the logic of your user program, which can include Boolean logic, counting, timing, complex math operations, and communications with other intelligent devices. (Siemens, 2016)

2.3.2 PLC Hardware

Siemens S7-1200 PLCs are compatible with the SPA function block and the one axis vector function block as well as Siemens S7-1500 series. It consists a power connector, memory card slot, removable user wiring connectors, status LEDs for the on-board I/O and a PROFINET connector. Fig. 8 shows S7-1200 PLC's appearance. (Siemens, 2016)

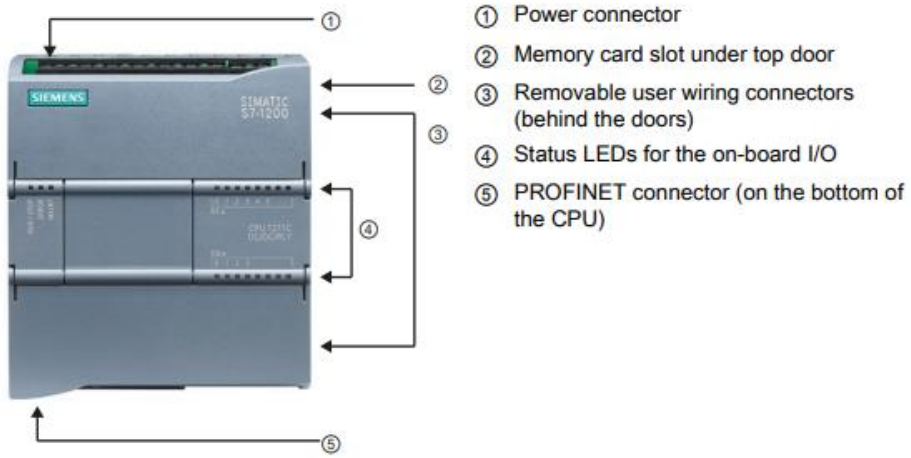

Figure 8. Physical appearance of Siemens S7-1200 PLC. (Siemens, 2016)

Siemens S7-1212 AC/DC/RELAY has eight 24 V DC digital input, six digital output relay 2A and two analog input 0-10 V DC. Table 7 shows the features of the Siemens S7-1212 AC/DC/RELAY. (Siemens, 2016)

Table 7. Features of the Siemens S7-1212 AC/DC/RELAY. (Siemens, 2016)

Feature	CPU 1212C
Physical size (mm)	90 x 100 x 75
User work memory	50 Kbytes
User load memory	4 Mbytes
User retentive memory	10 Kbytes
Local on-board digital I/O	8 inputs/6 outputs
Local on-board analog I/O	2 inputs
Process image size inputs (I)	1024 bytes
Process image size outputs (Q)	1024 bytes
Bit memory (M)	4096 bytes
Signal module (SM) expansion	2
Signal board (SB), Battery board (BB), or communication board (CB)	1
Communication module (CM) (left-side expansion)	3
Total high-speed counters	4 built-in I/O, 6 with SB
Single phase high-speed counters	0 at 100 kHz 1 at 30 kHz SB: 2 at 30 kHz
Quadrature phase high-speed counters	0 at 80 kHz 1 at 20 kHz SB: 2 at 20 kHz
Pulse outputs	4
Memory card	SIMATIC Memory card (optional)
Real time clock retention time	20 days, typ. / 12-day min. at 40 degrees C (maintenance-free Super Capacitor)
PROFINET	1 Ethernet communication port
Real math execution speed	2.3µs/instruction
Boolean execution speed	0.08 µs/instruction

2.3.3 Compact Switch Module

Siemens' compact switch module (CSM 1277) is used to establish connections between the devices in the system. This switch enables the PLC to communicate with the filed PG and the SIMATIC HMI panel. Start topology of the system can be seen in Fig. 9. (Siemens AG, 2010)

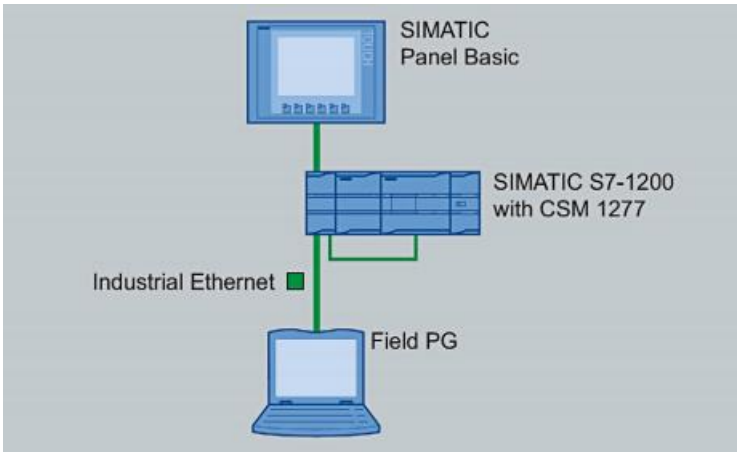

Figure 9. Star topology with the CSM 1277

CSM 1277 has four RJ-45 jacks for the connection of the end devices. Fig. 10 and 11 show the appearance of CSM 1277. (Siemens AG, 2010)

Figure 10. Compact Switch Module CSM 1277

Figure 11. RJ-45 jacks of the CSM 1277

CSM 1277 uses a 3-pin plug-in terminal block for power supply connection. The ground can be connected to the grounded DIN rail. Pin assignment for the power supply can be seen in Table 8. (Siemens AG, 2010)

Table 8. Pin assignments of the CSM 1277

Pin number	**Assignment**
Pin 1	L+ (24 V DC)
Pin 2	M (chassis ground)
Pin 3	Functional ground

Fig. 12 shows the place of the 3-pin plug-in terminal block on the switch module. (Siemens AG, 2010)

Figure 12. 3-pin plug-in terminal block on CSM 1277

2.3.4 Human Machine Interface (HMI)

Siemens SIMATIC HMI KTP700 Basic is a touch screen panel with a seven-inch display for the visualization of process control and monitor. It includes an USB port, seven function keys and an ethernet port for PROFINET interface. (Siemens, 2019)

Fig. 13 shows the design of Siemens SIMATIC KTP700 Basic. (Siemens, 2019)

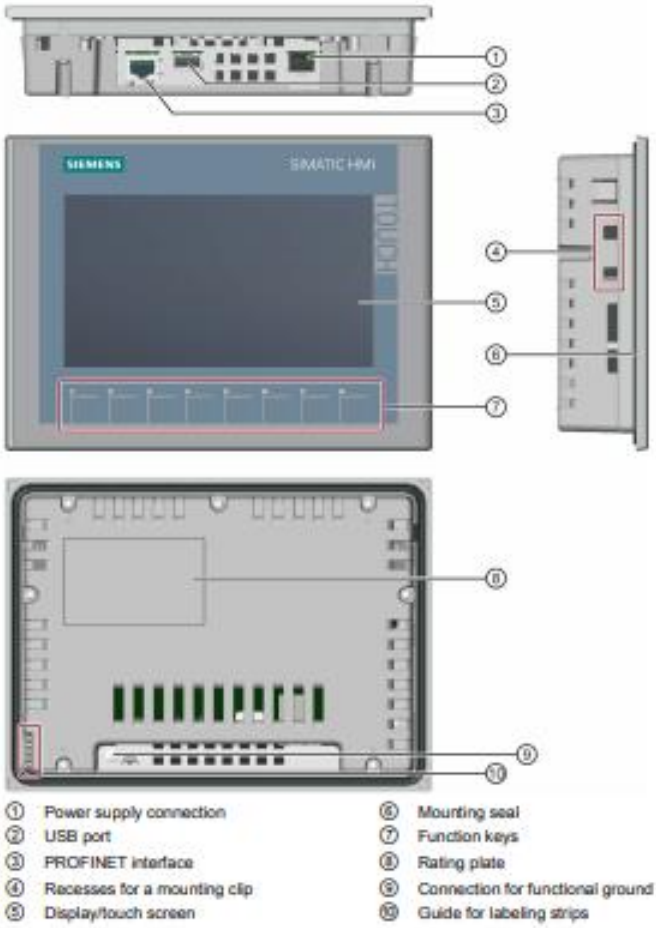

Figure 13. Design of Siemens SIMATIC KTP700 Basic. (Siemens, 2019)

2.3.5 Software

This project was configured with the Siemens SIMATIC STEP 7 (TIA Portal) Professional V15.1 programming software. This software stands as one of the world's most widely used software in industrial automation. TIA Portal features an integrated environment to configure PLC program and HMI visualization with a user-friendly interface. (Siemens, 2018)

2.4 **Motor**

The motor used to facilitate movement in the system was the RSPRO 177-4513, an electric 24VDC linear actuator. It had a 300mm stroke, and an IP protection rating of IP65. Fig 14 illustrates the motor. (RS Components Ltd)

Figure 14. RSPRO 177-4513 electric linear actuator (RS Components Ltd)

The motor is able to achieve linear motion by turning electrical energy into torque, which in turn moves the mechanism. This particular model has a max push/pull of 2000N, with speeds of 7.6mm/s and 5.7mm/s, when it has no load, and a full load, respectively. There is a total of five wires connecting from the motor. Two of them are for its power supply, and three for its feedback system as shown in table 9 below.

Table 9. Wire marking of the motor (RS Components Ltd)

Power		Signal		
Red	Black	White	Yellow	Blue
M+	M-	GND	VCC	Data

The motor also has a feedback system, where its position is communicated to the system via resistance or voltage rating between three wires, as shown in Table 9.

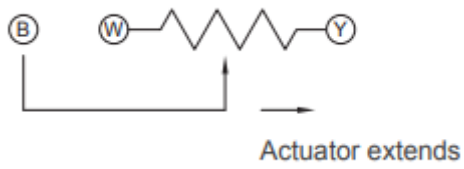

Figure 15. Resistance change in relation to actuator position (RS Components Ltd)

The yellow wire is supplied with 6VDC, while the white one is grounded. Figure 15 shows that when the actuator is extended, the resistance measured in the blue wire increases. At the same the voltage between the ground and the blue wire can be measured and compared to the voltage in the yellow wire to determine positioning. The measuring range of the PLC analog input is 0-10V, which is why voltage to the yellow wire must be limited to under 10 volts.

When positive power is supplied to the motors red wire, and negative power to the black one, the actuator will extend forward. In order to have it retract, an H-bridge, controlled by a PLC must be implemented, with the purpose of switching the polarity of the voltage applied. (see chapter 2.5)

2.5 **H-Bridge**

An H-Bridge is a component made of two relays, used to switch the polarity of a DC linear motor in order to cause it to move in reverse. When electricity flows from the positive pole to the negative one and then to the ground, forward movement is achieved and vice versa.

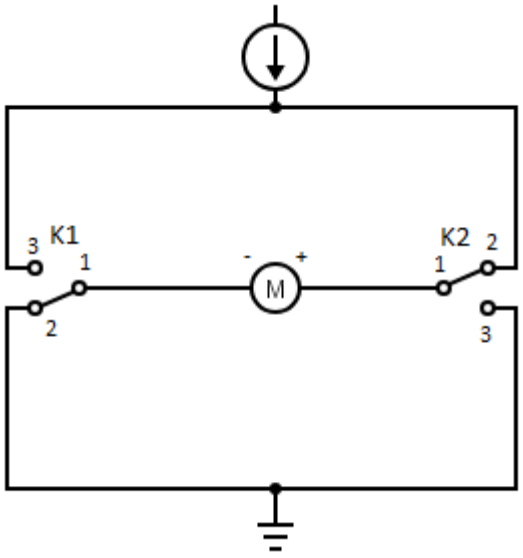

Figure 16. Circuit diagram of an H-Bridge

It is clear from Fig. 16 that two relays are needed. In the given example, the normal state of the relay has the pin 1 connected to pin 2. When the signal is given to the relays, they will switch their connection, linking pin 1 to pin 3, and allowing for the electricity to flow through the negative first, thus causing reverse movement.

3 IMPLEMENTATION

There are a number of methods to be implemented when creating a solar tracking system. This project was based on a closed loop system, with both single axis, and dual axis tracking. The system had two linear motors: motor A, set in the X-axis; and motor B, set in the Y-axis. The single axis method had one motor at a static position (motor B) and the other one (motor A), following the provided vector. The dual axis method obtained its tracking angles from the zenith and azimuth. Motor B utilized the elevation angle, which was derived from the zenith. The motor set in the X-axis however, had to track the sun horizontally by following the sun's azimuth. As explained below, this method is absent from the project and a different tracking system was used.

The single axis method utilized Siemens' function block to provide a tracking vector for the panel to follow. This was the Phi angle (see chapter 2.2.1) and it was 90° at sunrise and (-90°) at sunset. With these two setpoints the motor was programmed to be at a fully extended distance at sunrise, and at a fully retracted position at sunset. By dividing the rest of the space equally, accurate tracking was established. This method, however, assumes that a fully extended position of the panel would result to be at an angle of 90° relative to its middle position. In reality, the angle would be lower; thus, there would be a need for calibration.

Similarly, the elevation angle had a minimum and maximum setpoint, 0° at sunrise and sunset, and 90° at most during sun-transit. 0° to 90° are two realistic setpoints which the panel can follow after relevant calibration has been ascertained and applied.

The azimuth, which was needed for tracking by motor A, had an unrealistic tracking angle of 0 to 360°. It has no maximum or minimum points, and no reliable range to base motor movement on. Due to this, a different, more experimental tracking method was constructed. Siemens' TIA Portal application can generate sunrise and sunset times. This technique provided a start and endpoint for the motor to follow. The range provided here was taken from the longest day of the year, June 21st, giving the range of 13 to 83. This was to be the panels motion range, as all other shorter days would fall within this range.

3.1 PLC Program

The program itself was written in Function Block Diagram (FBD) language. It was divided into two main parts; the motor control system, and the solar tracking system. The solar tracking system generated the data necessary for the control system to direct and move the linear motors. As mentioned earlier, there were two methods of tracking in this program: dual axis, and single axis.

The single axis tracking method was done through two function blocks. The first one was SPA_Calc_SunVector (see chapter 2.2.1), which through the inputs of the longitude, latitude and other parameters mentioned in Table 2, generated the azimuth and zenith of the sun in a particular location. These two datapoints would then have to go through the CalcOneAxisVector function block (see chapter 2.2.1), which would subsequently

calculate the ideal tracking vector of the panel for the sun, thereby generating what is known as the “Phi” angle. This vector is the desired angle which the panel must simulate, by means of extending the linear motor; thus, resulting in the panel tilting to one side, and retracting it for the opposite effect.

When single axis tracking is enabled, the control system will run through a number of steps before movement can commence. The first step is to check what is the current tracking mode of the system (see chapter 3.1.6). Constant refers to the constant tracking mode, in which the motor will move when the PHI angle is two degrees or more removed from the panel angle. Timed tracking refers to periodic tracking which can be set from the user from the human machine interface (HMI). As an example, the user can set a five minute during which tracking is turned off, and a 45 second window for the motor to go to the right position; after which the process restarts. If the system is in constant mode, then it will check the data provided by the tracking system and compare it to the real position of the panel. From this point there are four possible outcomes. If an error occurs in the tracking system, the panel will move towards the middle position until the error is cleared. Two other possibilities are the real angle being below or above the targeted angle. When this is true the motor will either extend or retract to the right position. If after the angle comparison the PHI angle matches the panel angle, then the process is repeated until this is not true. Timed mode has the same outcomes with the extra step of waiting for the timer to expire prior to commencing any movement measures.

If tracking is set to dual axis the system functions very differently. In this case the tracking system must provide each motor with its own setpoint. For the Y-axis motor (motor B), it gives the elevation angle, derived from the zenith. For the X-axis motor (motor A) it gives a time of day setpoint, which is later compared to the minimum and maximum points for that day (sunrise and sunset), and provides a number in the -90 to 90 range corresponding to the true angle of the sun.

Contrary to the single axis system, the dual axis setup has no modes from which to choose from, all tracking is constant. When the setpoint values are presented from the tracking system, the control will compare both motors’ position and lead to one of the same four outcomes as in the single axis mode. Figure 17 shows a flowchart of the system’s decision-making process.

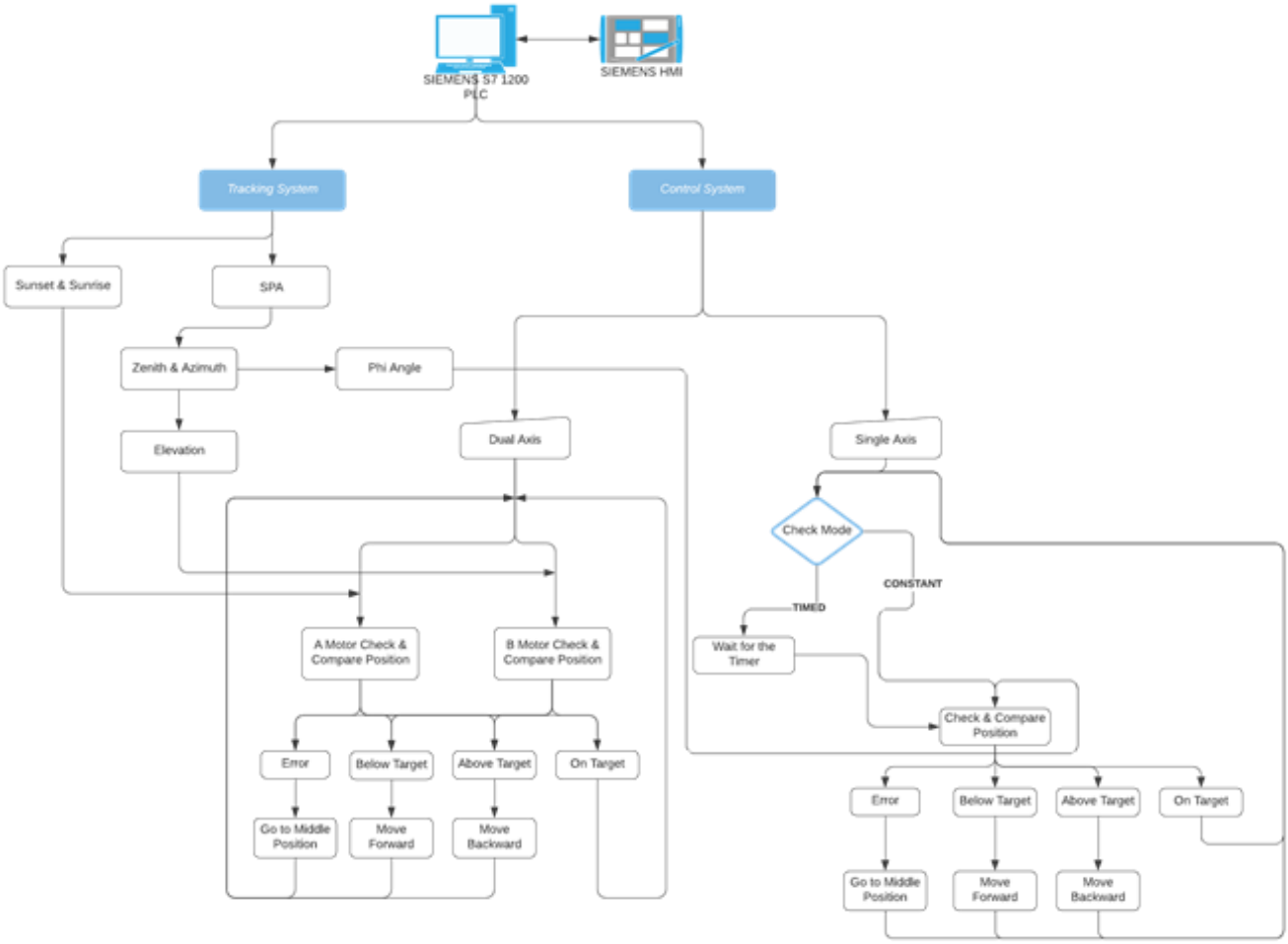

Figure 17. PLC program flowchart

3.1.1 Networks

The system functions as the PLC reads through the networks that are being called in the OB1 organization block. OB1 organization block consists of function blocks and common programming commands. While most of the networks are explained in the following chapters, Figure 18 shows a graph of the division of the networks for the autonomous solar panel movement. The arrows between some of the networks indicates their association with each other.

OB1 starts its process with the “Data collection” networks. These networks stand as the key elements of the system to get the essential data such as azimuth, zenith and, phi angles. Configuration complexity of the movement modes for the system can be seen under the titles of “Manual Movement”, “Constant Automatic Movement”, “Set Degree Movement” and, “Timed Movement”. HMI display has been configured through number of networks, which can be seen under the “HMI Display Configurations”. As opposed to motor A’s configuration, motor B has built by its own function block. However, the motor B function block is still being called at the OB1 organization block.

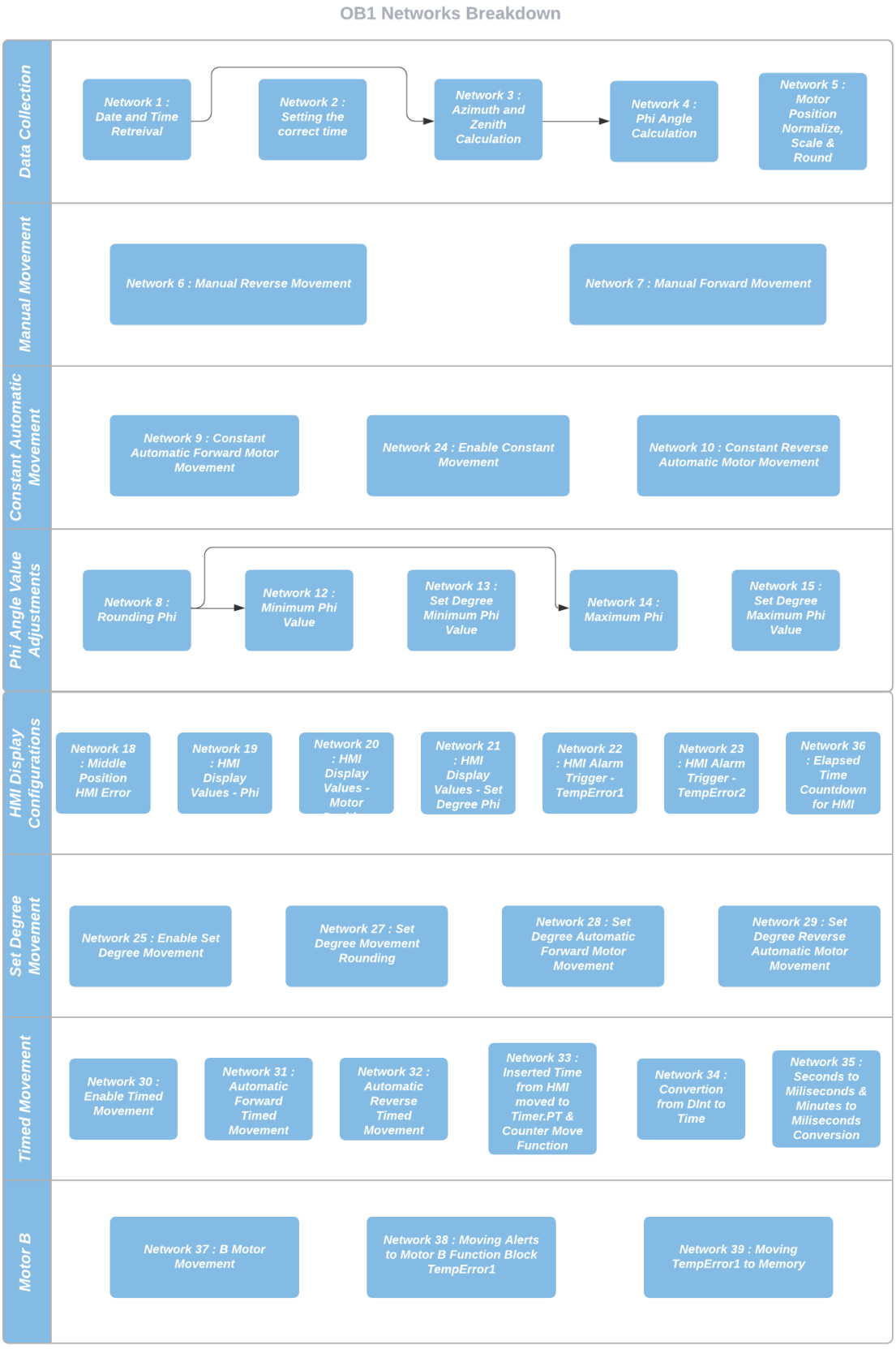

Figure 18. Breakdown of the OB1 Networks

3.1.2 SPA Function

The function (SPA_CalcSolarVector) is built by Siemens as a know-how protected function and calculates the solar azimuth and zenith values which are subsequently used in the phi angle calculation (see chapter 3.1.3). The inputs of the function are UTC (Universal time coordinated), longitude, latitude, pressure, temperature, elevation, delta_T, and atmospheric refraction, as shown in figure 19). If any of the input variable parameters are off of its supposed range then the output #tempError_1, switches to state 1 from state 0 which is later in the program used to configure a global error.

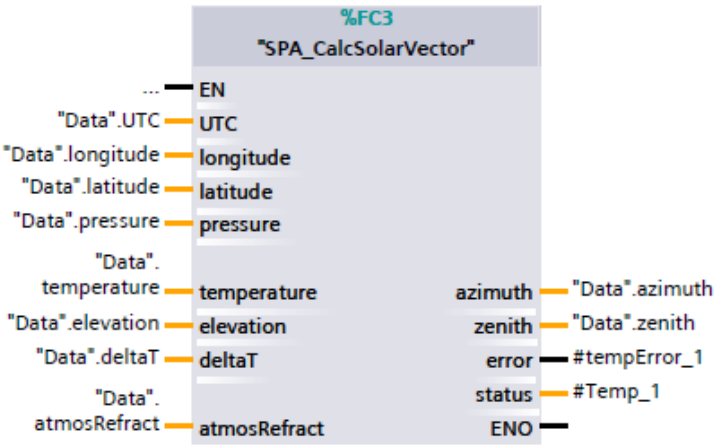

Figure 19. SPA_CalcSolarVector function in Siemens TIA Portal

3.1.3 One Axis Vector Function

This function calculates the phi angle which stands for the most effective angle of tracking for the panel. The phi angle output is utilized by the motor A to for single axis movement. The function is built by Siemens and is know-how protected. It uses ten inputs to calculate the phi angle which can be seen in the figure 20 below.

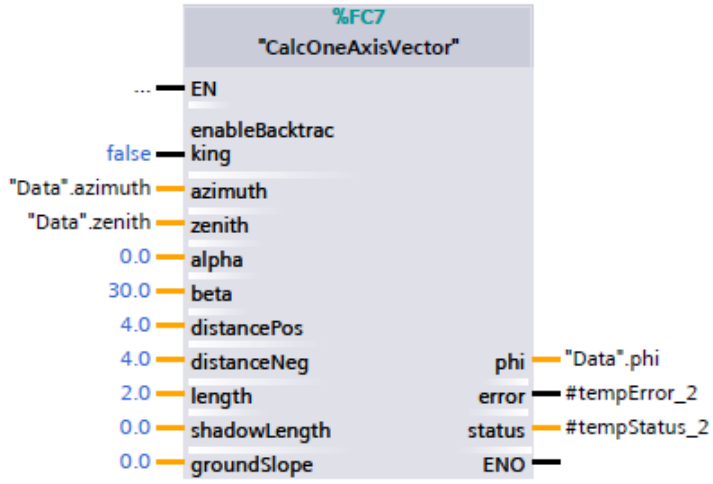

Figure 20. CalcOneAxisVector function in Siemens TIA Portal

3.1.4 Positional Feedback of Motors

Integration of the motors' positional feedback is configured by several functions that is supported by Siemens TIA Portal, can be seen in the figure 21. The resistance values that is received from the motors are read as an integer type in the inputs of the PLC's I/O module. Then, this value is converted to a real type before it is rounded up to avoid rapid changes in the potentiometer. Then, the rounded value gets scaled down into the range of -90 to 90 to fit the range of the phi angle. At last, the scaled value gets rounded once again to attain a stable positional value in the scale of -90 to 90.

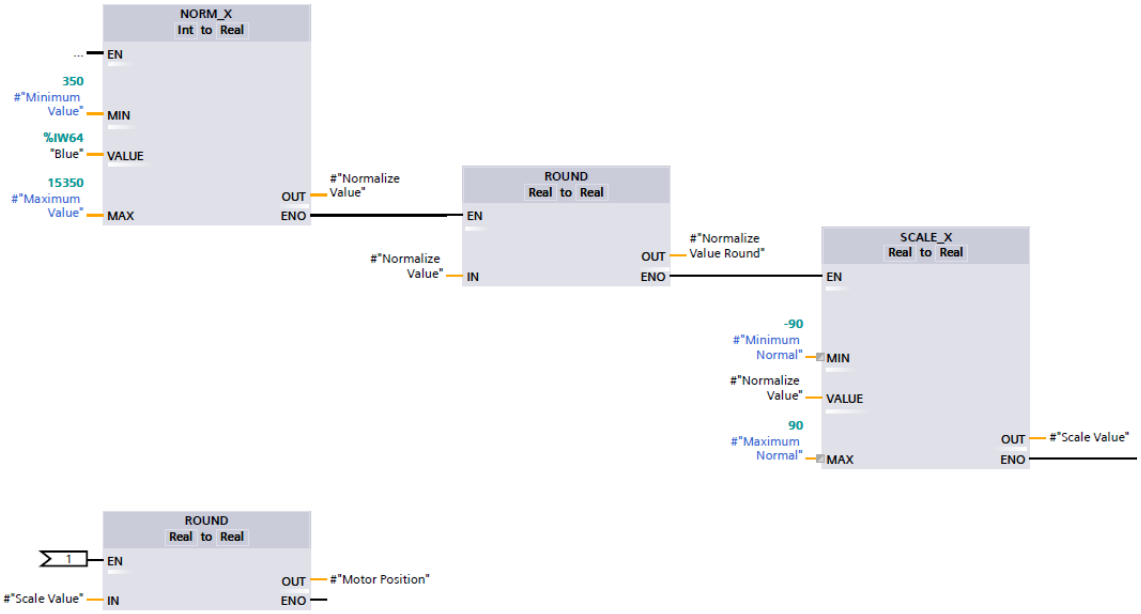

Figure 21. Network for the Motor Position Normalize, Scale & Round

3.1.5 Manual mode

The motors have two different modes. One is manual mode and the other one is automatic mode. A set-reset function is used to switch between the two functions. The motor starts moving forward as the "Move Motor Command" is at state of 1 and it moves reverse as the "Reverse Command" is at the state of 1. The networks for forward and reverse movement can be seen in the figure 22 and figure 23 below.

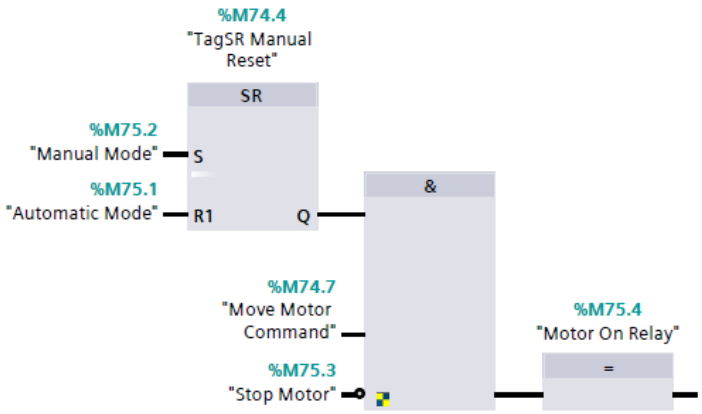

Figure 22. Manual forward movement network

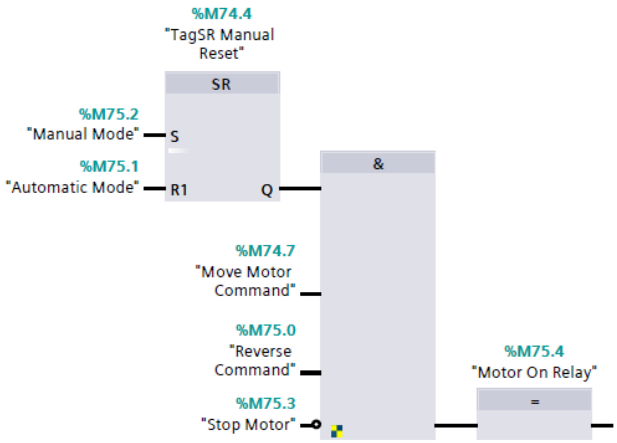

Figure 23. Manual reverse movement network

3.1.6 Single Axis Automatic Modes

Single axis tracking is built with different methods. The one described as “constant automatic mode” has two separate networks to move in two directions.

Forward movement network works with relatively simpler logic compared to reverse movement. The logic works behind an SR function where a compare function set the SR function. The compare function compares the values of the “Phi” and the “Motor Position” to set the SR function if the “Phi” value reads higher than the “Motor Position” which activates the “Forward Relay” relay for motor to turn on and, consequently move forward. An In-range function activates the “Stop compare” assignment if the “Motor Position” value is between “Minimum Phi” and the constant value of 180 which is one of two inputs of the or function that triggers the reset of the SR function which eventually stops the motor. The network configuration can be seen in the figure 24 below.

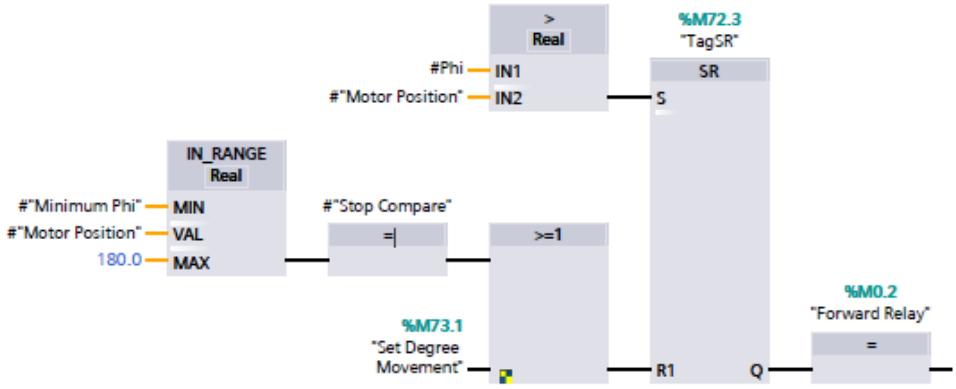

Figure 24. Network 9: Constant Automatic Forward Motor Movement.

Due to the nature of the H bridge connection that is used to execute the reverse movement of the motor, the “Constant Reverse Automatic Motor Movement” network has a more complicated logic compared to forward movement network. The structure of this network can be seen in the figure 25 below.

The motor moves in reverse direction only if the “Reverse Movement Relay” is turned on. Reverse movement motor can be activated under different conditions. This relay would be activated if:

- The “Set degree Reverse Movement Relay” is on and the “Manual Mode” is off.
- The “Manual Mode” and “Reverse Command” is on.
- The “Manual Mode” is off and the “Timed Reverse Movement Relay” is on.

In addition to, when the “Set Degree Movement” and “Enable Timed Movement” is off when the “Automatic Mode” is on and if the “TagSR Trigger Reverse” SR function is set an output or if there is an error in the system.

The “TagSR Trigger Reverse” SR function sets the output on when the compare function compares the values of the “Phi” and the “Motor Position” to set the SR function (“TagSR Reverse”) if the “Phi” value reads higher than the “Motor Position”.

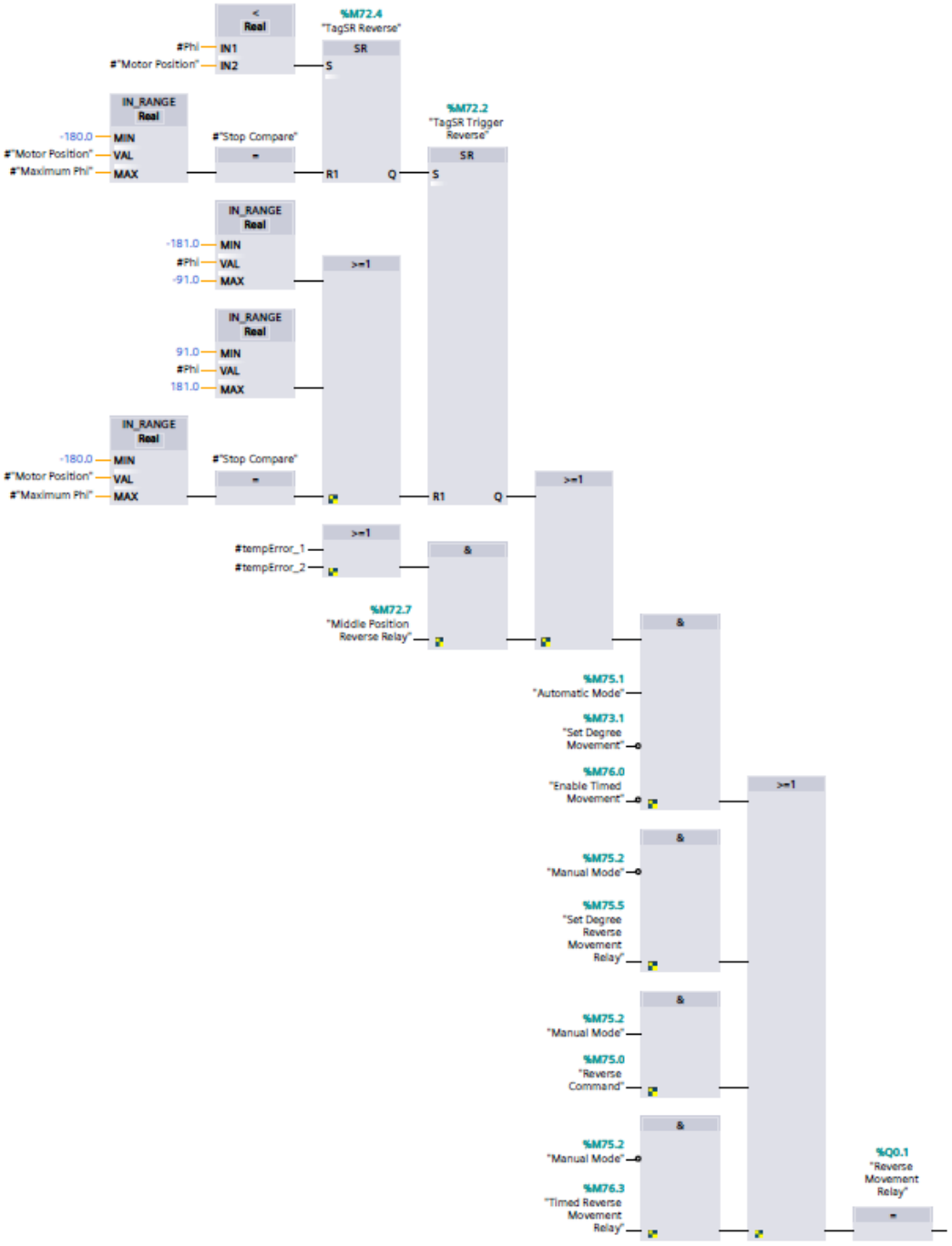

Figure 25. Network 10: Constant Reverse Automatic Motor Movement

3.1.7 Minimum and Maximum Phi Values

It has been designed to configure two additional values of the phi value in the system to be used in range checks either stop or continue to comparing values for automatic movement. These two values were configured by simply using SUB(subtraction) and ADD(addition) functions. Below you can see the two networks in figure 26 and 27.

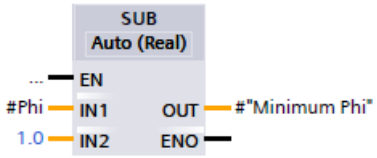

Figure 26. Network 12: Minimum Phi

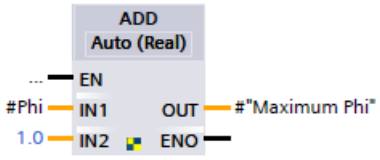

Figure 27. Network 14: Maximum Phi

3.1.8 Alarms Triggered by Calculation Errors

There are two alarms configured in the system. These are an indicator of a malfunction in the two main functions of the system, SPA_CalcSolarVector function (azimuth and zenith calculation) and, CalcOneAxisVector function (phi angle calculation). If the azimuth and zenith calculation function has an incorrect input value then the state of the "#tempError_1" output is set to 1. Likewise, if the phi angle calculation function happens to have an incorrect input value then the state of the "#tempError_2" is set to 1. These alarms are being displayed in the HMI and, trigger assignments for the error state solutions of the system. Data types of the alarms can be seen in the figure 28 below.

Name	Data type
Temp	
tempError_1	Bool
Temp_1	Word
tempError_2	Bool
tempStatus_2	Word

Figure 28. Data types of the alarms of the SPA_CalcSolarVector function and the CalcOneAxisVector function

3.1.9 Error Triggered Actions

The program built in a way that if either of two calculation errors is on then motor A will go to the middle position until the errors are cleared. This is built to keep the panels in range in case of a long-running error. This network's configuration can be seen in the figure 29 below.

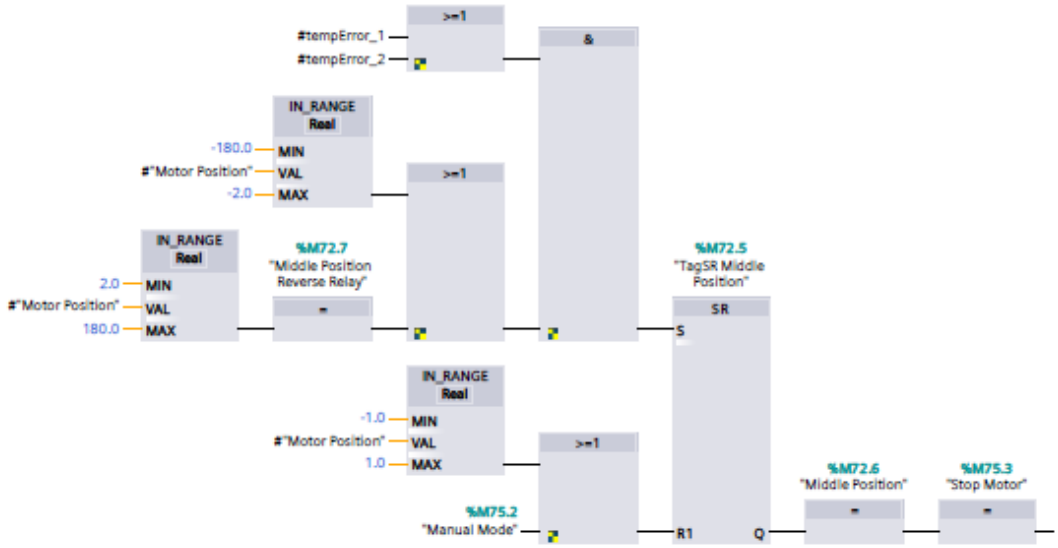

Figure 29. Network 17: Error triggered Middle Position Movement

3.1.10 Enabling Automatic Modes

There are three different automatic modes of operation programmed. The user can select either one of these modes for system to operate. This selection process works behind a simple AND function configuration. Networks for constant movement and the set degree movement modes can be seen in the figure 30 and figure 31 below.

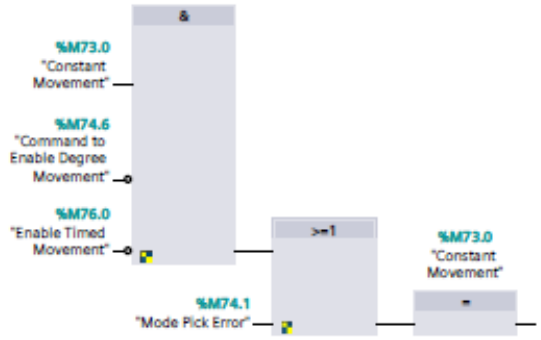

Figure 30. Network 24: Enable Constant Movement

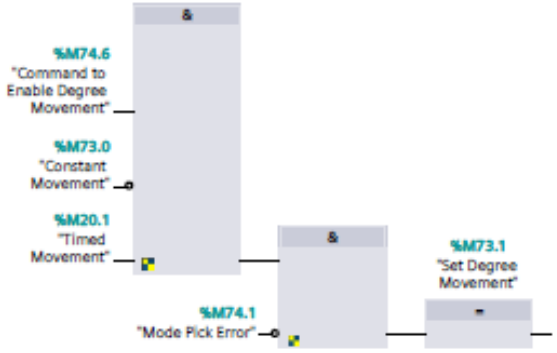

Figure 31. Network 25: Enable Set Degree Movement

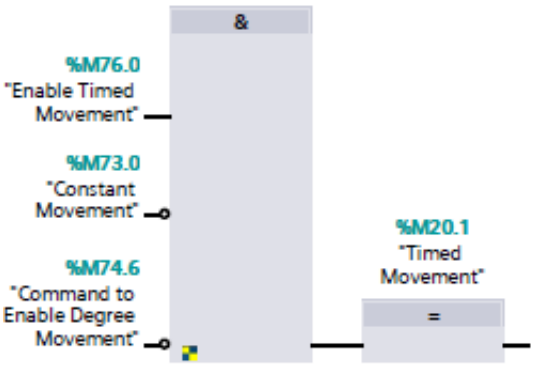

Figure 32. Network 30: Enable Timed Movement

Also, when two or more modes are on at the same time the error “Mode Pick Error” is active. When this is true motor movement defaults back to "Constant Movement". This network can be seen in the figure 33 below.

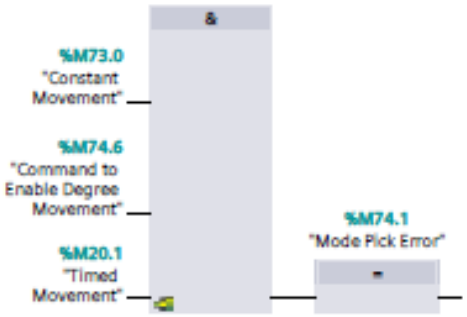

Figure 33. Network 26: Mode Error

3.1.11 Automatic Timed Movement

Automatic timed movement mode has two networks configured for its movement. One for forward movement and one for reverse movement. This mode has an IEC Timer built in addition to the range check and compare functions. The difference between its forward and the reverse movement can be seen in the figure 35 and figure 36 below. In this mode, the operator (user) can input the intended time for motor to move at intervals from the HMI screen. The configuration of this function can be seen in the figure 34 below.

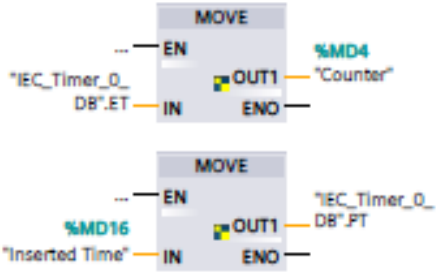

Figure 34. Network 33: Inserted Time from HMI moved to Timer.PT & Counter Move Function

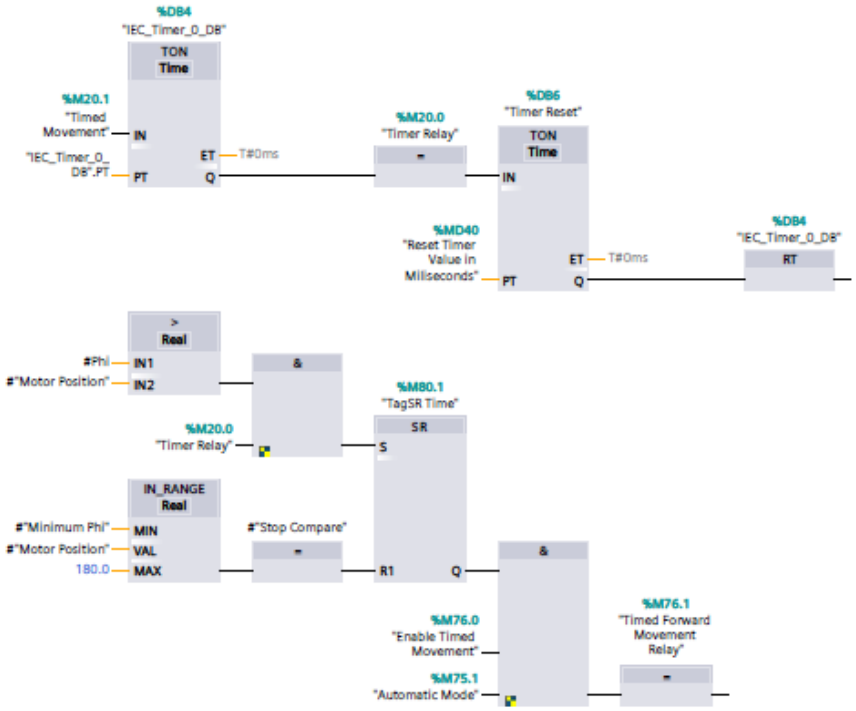

Figure 35. Network 31: Automatic Forward Timed Movement

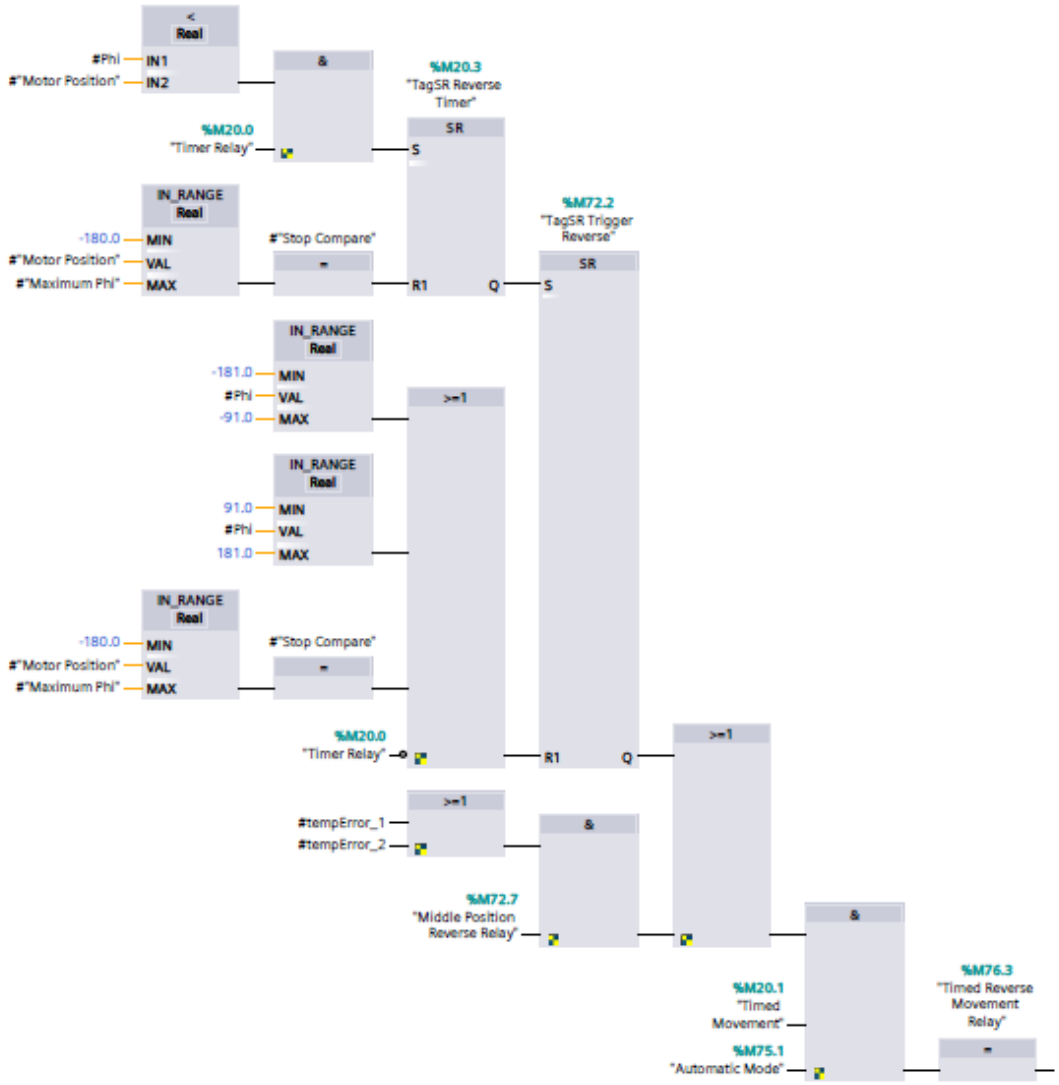

Figure 36. Network 32: Automatic Reverse Timed Movement

The motor moves in reverse direction in the Timed Movement only if the “Timed Reverse Movement Relay” is turned on. This relay is activated in the following circumstances: when the “Timed Movement” and the “Automatic Mode” on while either there is an error in the system or the “TagSR Trigger Reverse” has an output.

The “TagSR Trigger Reverse” SR function sets the output on when the compare function compares the values of the “Phi” and the “Motor Position” to set the SR function (“TagSR Reverse Time”) if the “Phi” value reads higher than the “Motor Position”.

Also, the elapsed time until the motor's next movement can be seen in the HMI screen. This is configured with the T_SUB function with the addition of T_CONV function to visualize it on the HMI screen and, can be seen in the figure 37 below.

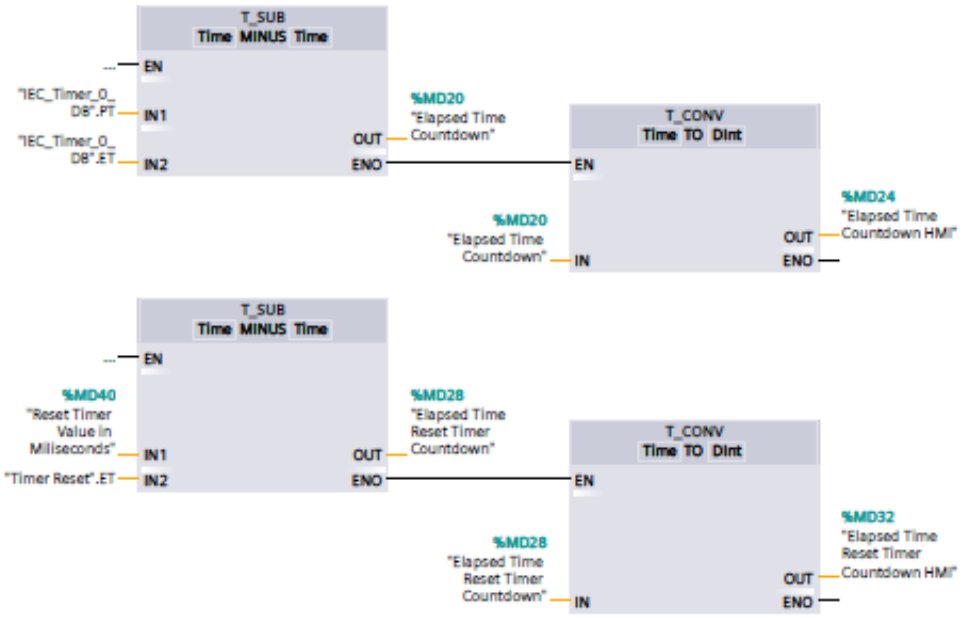

Figure 37. Network 36: Elapsed Time Countdown for HMI

3.1.12 Morning Position

After sunset panel will automatically return to morning position in anticipation of the next sunrise. If the calculated phi value from the "CalcOneAxisVector" is between the ranges of -181° … -91° and, 91° … 181° then the "Morning Position Command" assignment will be triggered to command motor to move to the morning position. The logic of this network can be seen in the figure 28 below.

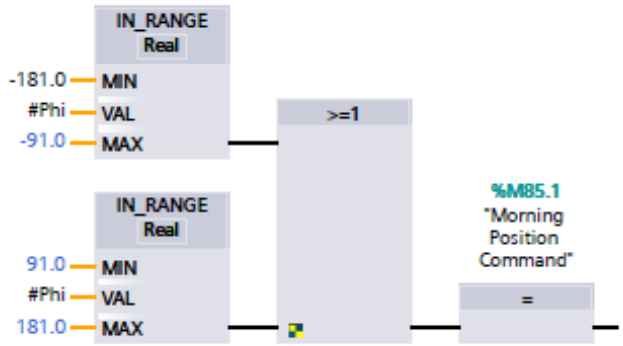

Figure 38. Network 16: Return to morning position

3.1.13 Range Checks

Due to the nature of the motor feedback system (motor is not very accurate) all positions of the motor have an accuracy of ±1°. This means that if the desired angle is 30°, motor might be at 29° or 31° depending from which end it approaches. If this is not implemented, motor can overshoot and trigger the PLC circuit breaker.

3.1.14 HMI Setup

HMI display of the system has two screens for user to operate through two motors of the system. First screen is designed to control the motor A and, display its vital values. Full screen view of the screen can be seen in the figure 39 below.

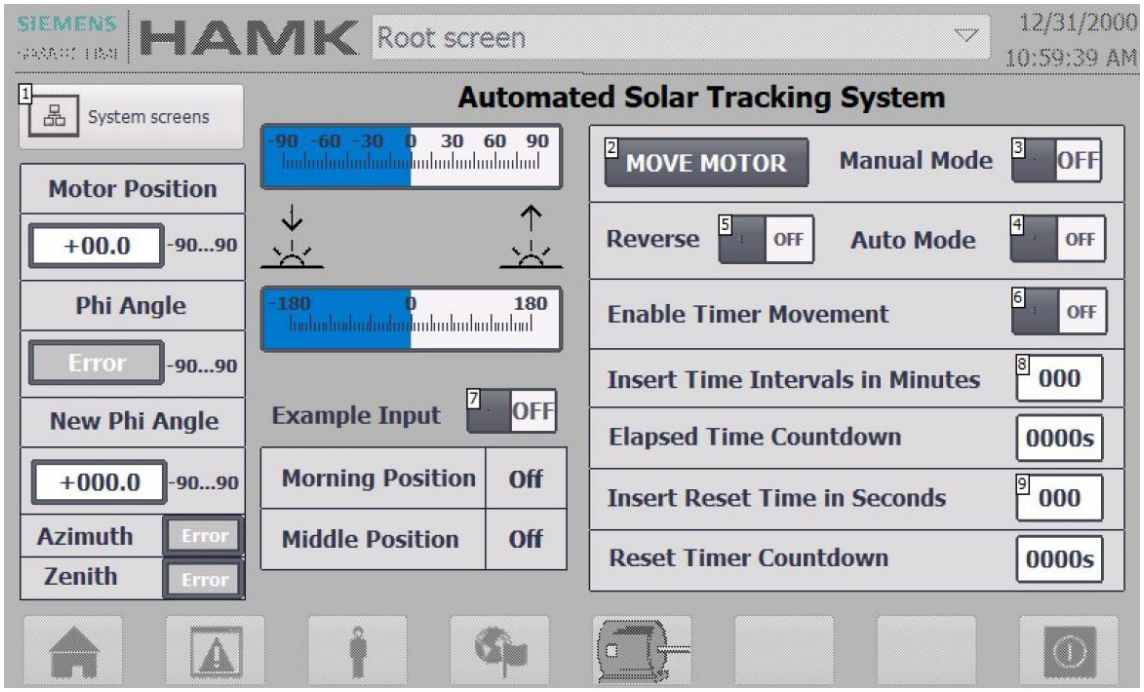

Figure 39. Motor A screen

Below the figures 40, 41 and, 42 explains the role of the buttons and process value fields.

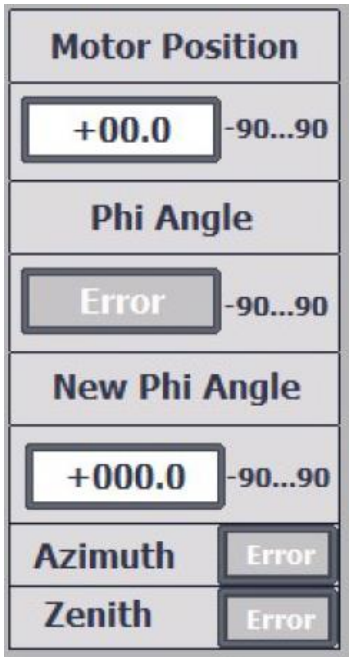

Displays the motor position value between -90° and 90°

Displays the phi angle value between -90° and 90° also indicates if there is an error regarding the phi angle calculation

Displays the updated phi angle value between -90° and 90°

Displays the phi angle value between -90° and 90° also indicates if there is an error regarding the phi angle calculation

Figure 40. Main screen information centre

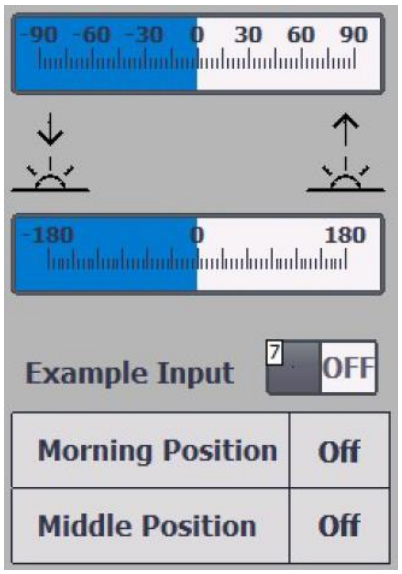

Displays the positional values of the motor A between -90° and 90° and, the motor B between -180° and 180°

Indicates if the Morning Position mode and the Middle Position mode are on or off

Figure 41. Motor state and positional values

Moves the motor forward and backward

Turns on the manual movement mode

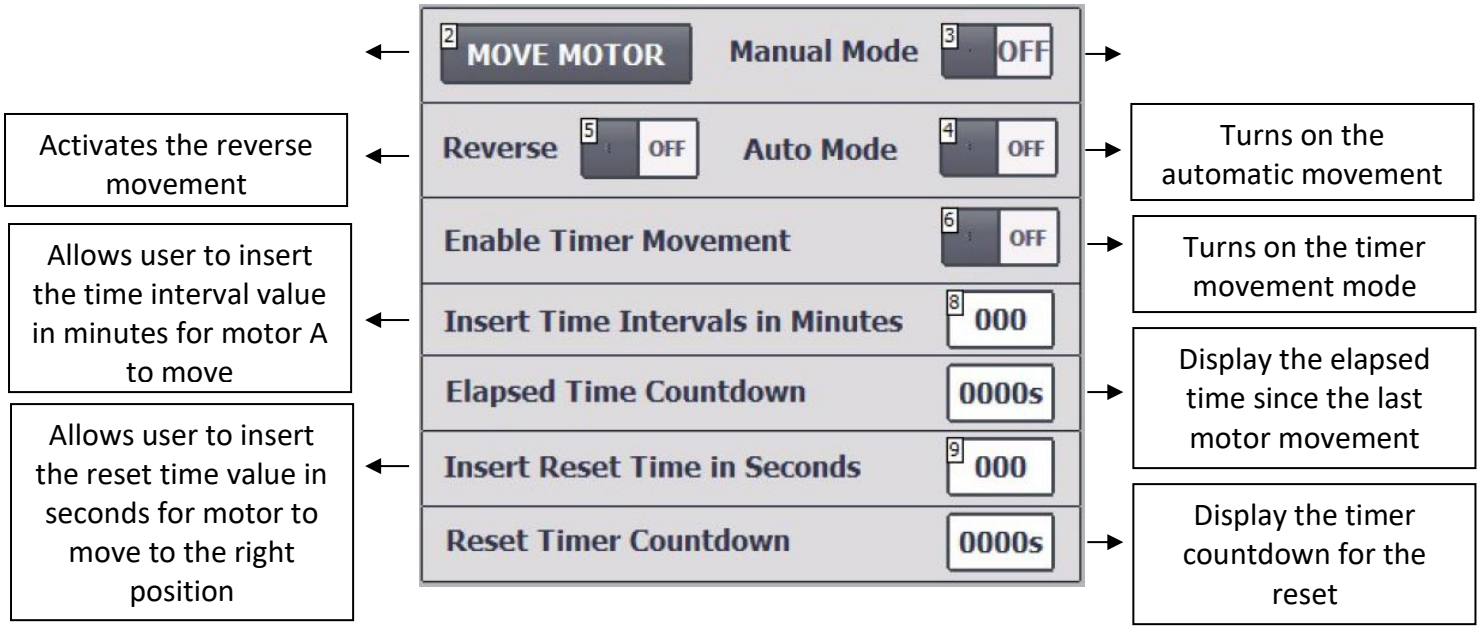

Figure 42. Motor screen command centre

The second main screen is configured to control the B motor (Y-axis). It is also possible to control the Dual Axis settings on this page. Full screen view of this page can be seen below in the figure 43.

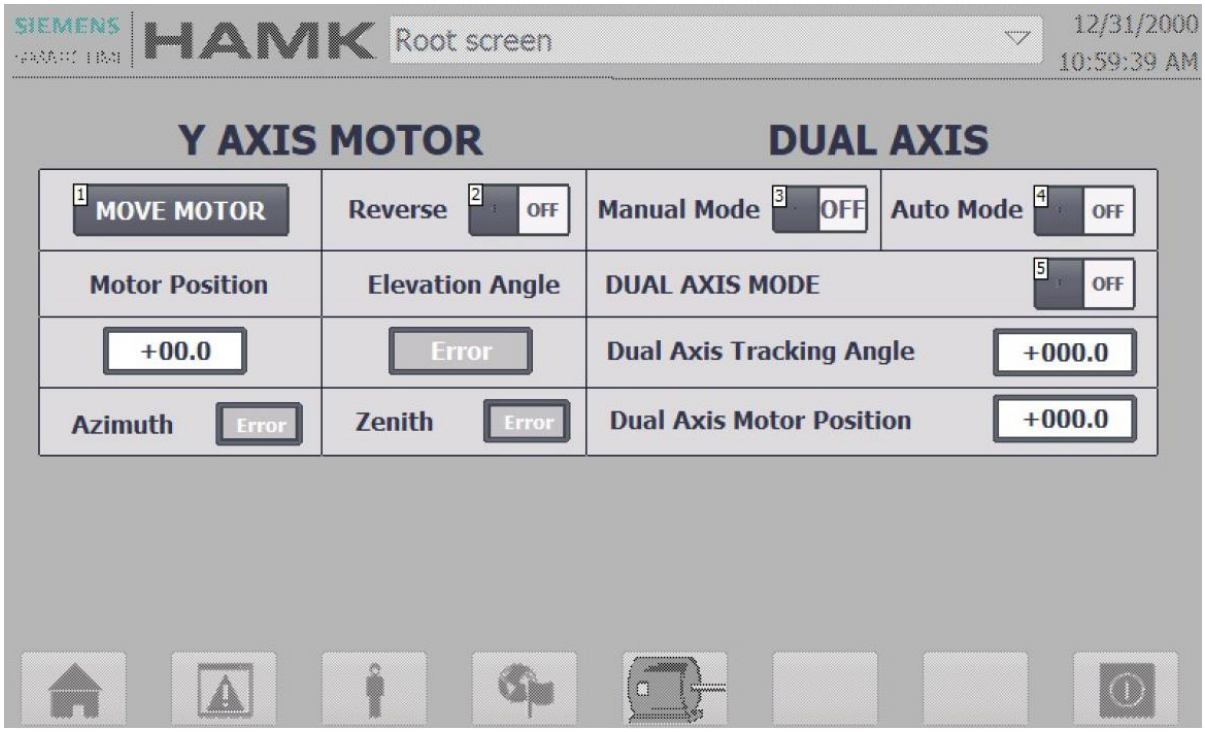

Figure 43. Motor B and Dual Axis Control Screen

Figures 44 and, 45 explains the role of the buttons and process value fields.

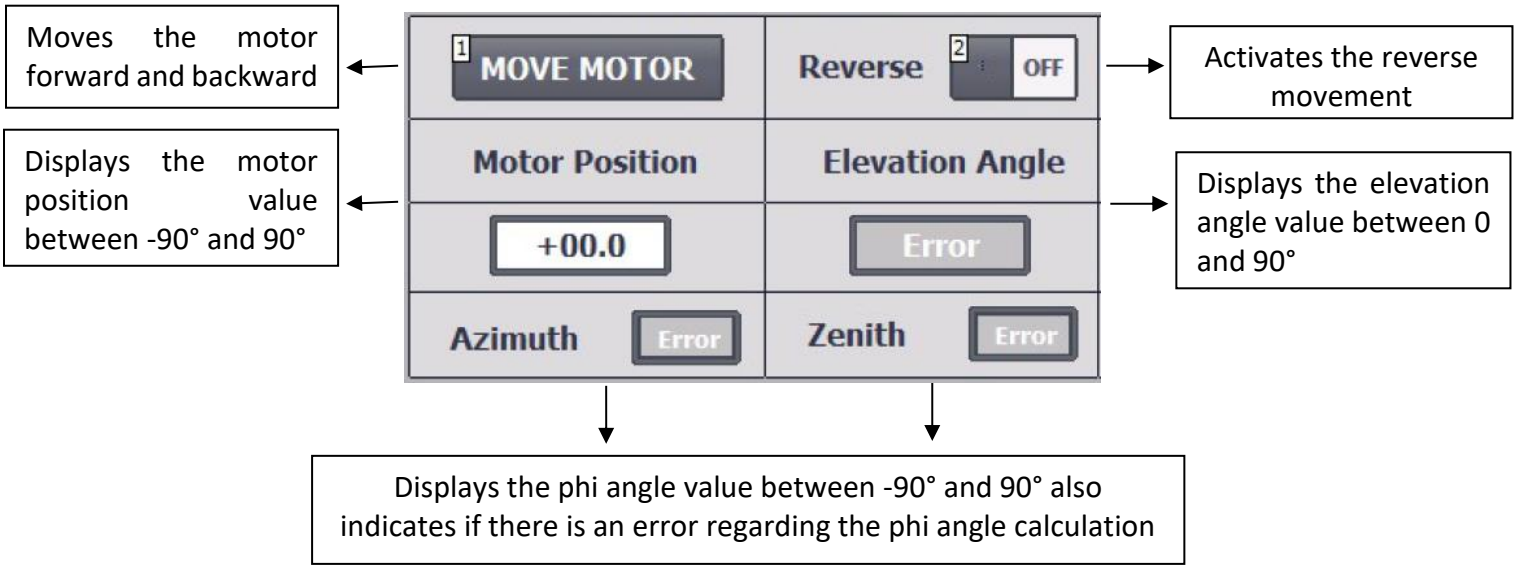

Figure 44. Y-Axis Motor Information Display

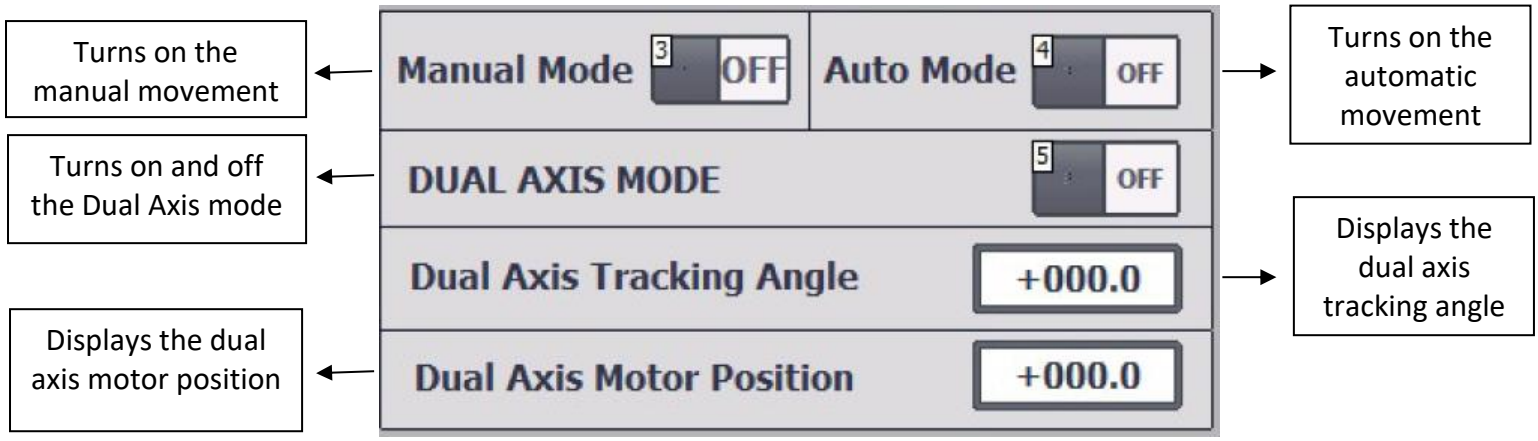

Figure 45. Dual Axis Information Display

3.2 **Hardware Configuration**

The hardware components used in this project are listed below:

- Siemens S7-1212 AC/DC/RELAY PLC
- Compact Switch Module CSM 1277
- Siemens SIMATIC KTP700 Basic HMI
- Voltage regulator (x2)
- RSPRO 177-4513 Electric Linear Actuator
- Relay Switch (x6)
- 24VDC Power Supply

The system's control unit was the S7 PLC, the switch module acted as a gateway for the PLC to PC and PLC to HMI connection via an ethernet cable. The motors had five wires,

two of which were power wires connected to the power supply after passing through relay switches. Four of the relay switches formed an H-Bridge which was triggered from the PLC when reverse movement was needed. Similarly, the other two relay switches controled the flow of electricity from the power supply to the motors and are activated by the PLC. The motors' feedback system went through the voltage regulators to lower the voltage from 0-24VDC to under 0-10VDC and links to the PLC's analog input connection.

3.2.1 PLC Cabinet

The PLC cabinet included four main components, which are listed below:

- Siemens S7 1212C AC/DC Relay CPU
- CSM 1277 Simatic Net Switch Module
- Terminal Blocks
- Switch Relays

The CPU was fed 240VAC from either a power supply or an outlet, and it was converted to 24VDC. This supplied power to the switch module and the HMI screen. The former was used as a bridge connection between the PLC, PC, and HMI via ethernet cable. There were also a number of terminal blocks to facilitate the needed grounding and connections for the system's components, in addition to switch relays for surge protection and reverse movement. Figure 46 below shows the schematics of the cabinet layout. The HMI screen was not included into the drawing as it was positioned outside the box.

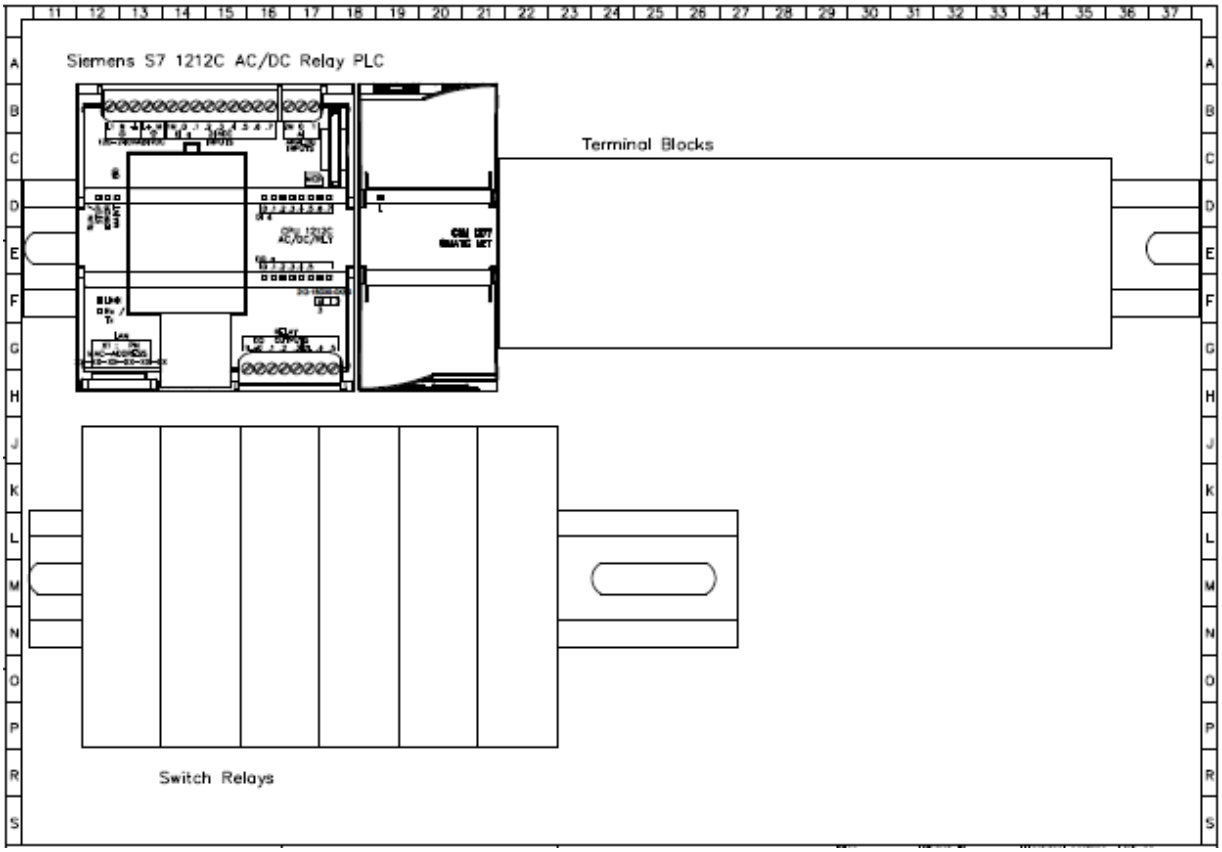

Figure 46. Cabinet layout drawing

4 RESULTS AND ANALYSIS

This chapter pertains to the results of the hardware configuration and programming of the system, as well as a theoretical analysis on the value and significance of establishing solar tracking systems.

In the genesis of this project, the goal was to design an autonomous solar tracking system in order to compare its power yield to a static panel system. Afterwards, the data received was to be processed, with the end goal being an empirical analysis of the system's performance and effectiveness. Due to the COVID-19 situation in Finland during the writing of this thesis (Finnish Institution for Health and Welfare, 2020), implementing the project as planned proved to be difficult. As such, the analysis of solar tracking systems and their effectiveness was done by examining various publications that tackle the subject.

4.1 Data Analysis

The main challenge when implementing solar tracking systems is an economical one. The initial cost of the tracking system with motors, movable joints, and a control unit, can significantly increase the capital investment. In order to better understand the risks associated with such systems, a detailed analysis is essential.

4.1.1 Comparison of Dual Axis Tracking Against a Fixed PV System

There are a number of published research papers that compare the effectiveness of these systems. One such research project conducted and published in Turkey, draws a parallel between dual axis tracking and fixed systems, determining that there is a 30.79% increase in the electricity obtained from the dual axis tracking photovoltaic system compared to the fixed photovoltaic system. Figure 47 shows two graphs which represent the energy gained from implementing a tracking system during a high and low irradiation month respectively. This set of data clearly shows the effectiveness of a dual axis system during non-peak sun hours, highlighting the loss of energy from static panels due to panel positioning. (Eke & Senturk, 2012)

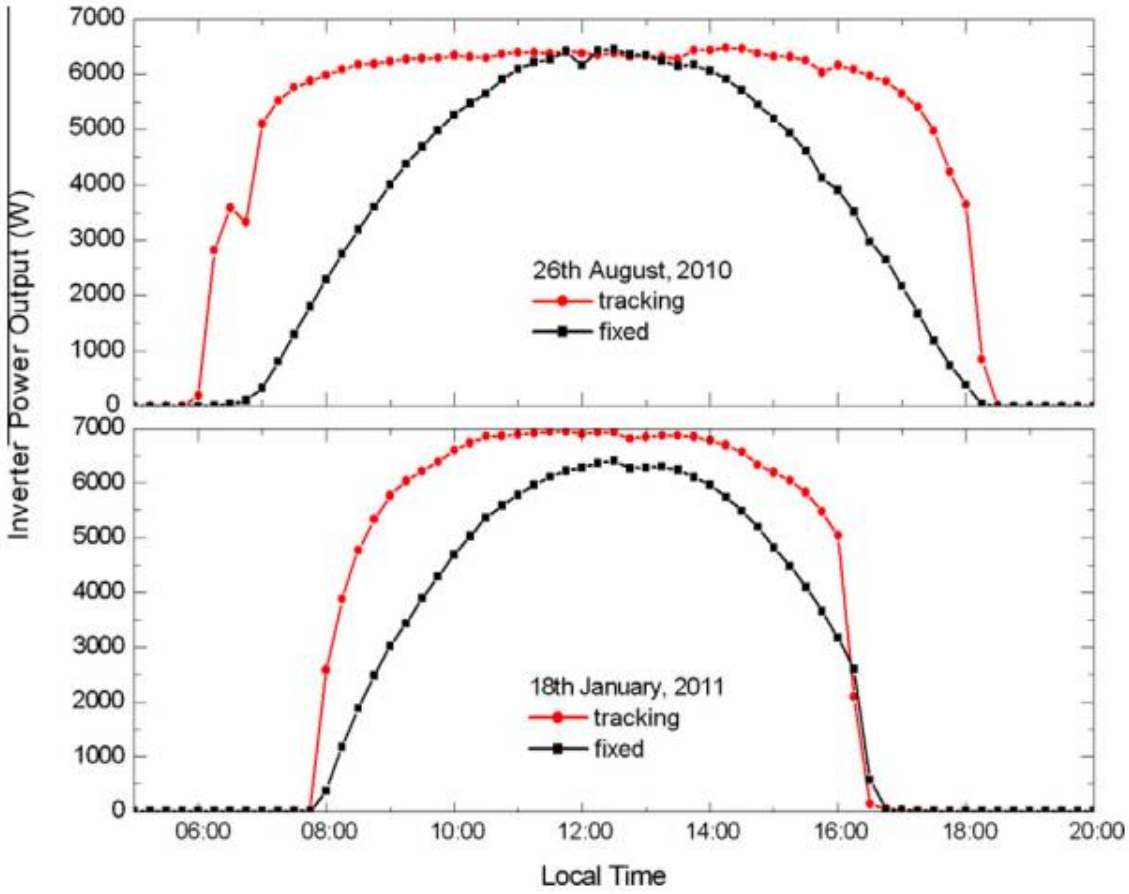

Figure 47. Photovoltaic systems power yield (Eke & Senturk, 2012)

An observation that can be made from Figure 47, is the impact of irradiation on the effectiveness of the system. In months with higher irradiation from the sun, the gain percentage trends higher. Table 10 shows the monthly yield and gain of the dual axis tracking system, and a correlation between the two.

Table 10. Monthly yield and energy gain of the double axis tracking PV system. (Eke & Senturk, 2012)

Month	Fixed System (kWh/month)	Tracking system (kWh/month)	Gain (%)
January	53.49	62.56	16.96
February	78.29	92.50	18.15
March	147.75	181.11	22.58
April	157.65	209.32	32.78
May	166.80	229.90	37.83
June	144.80	206.26	42.44
July	152.67	209.92	37.50
August	152.67	209.92	37.50
September	165.16	215.63	30.56
October	107.31	131.12	22.19
November	92.48	113.10	22.30
December	41.45	49.40	19.18

In Table 10, it can be seen that despite the variation in the gain percentage throughout the year, it is still significant enough to support the implementation of a tracking system. The above-mentioned variation can be better visualized in Figure 48, which shows a spike in efficiency in the high irradiation period of May to August.

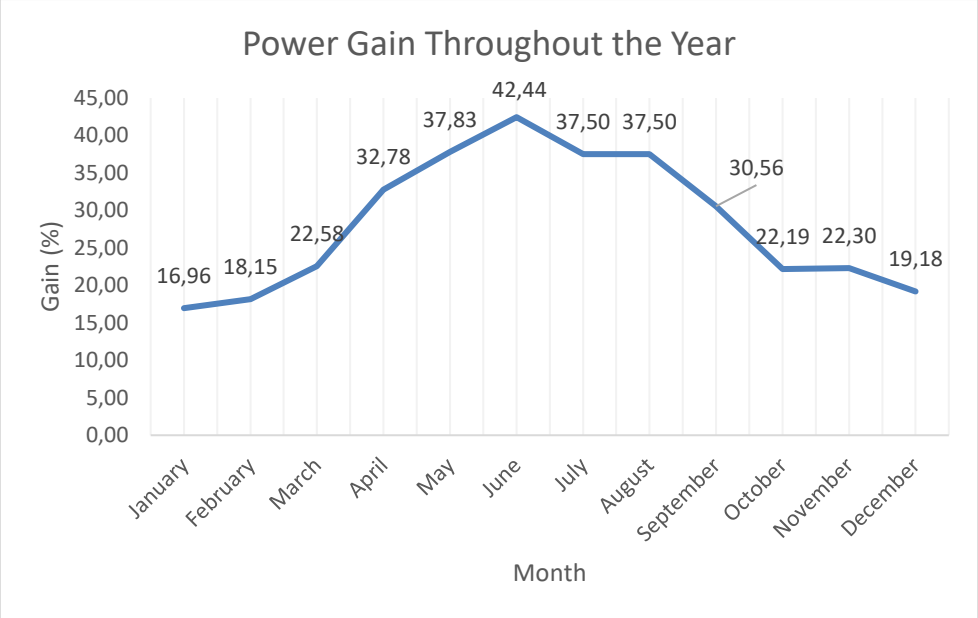

Figure 48. Dual axis tracking system power gain throughout the year. (Eke & Senturk, 2012)

Results from another paper studying the effect of dual axis tracking as compared to single tracking supports the idea of the former being more efficient in the summer months as seen in Figure 49 below.

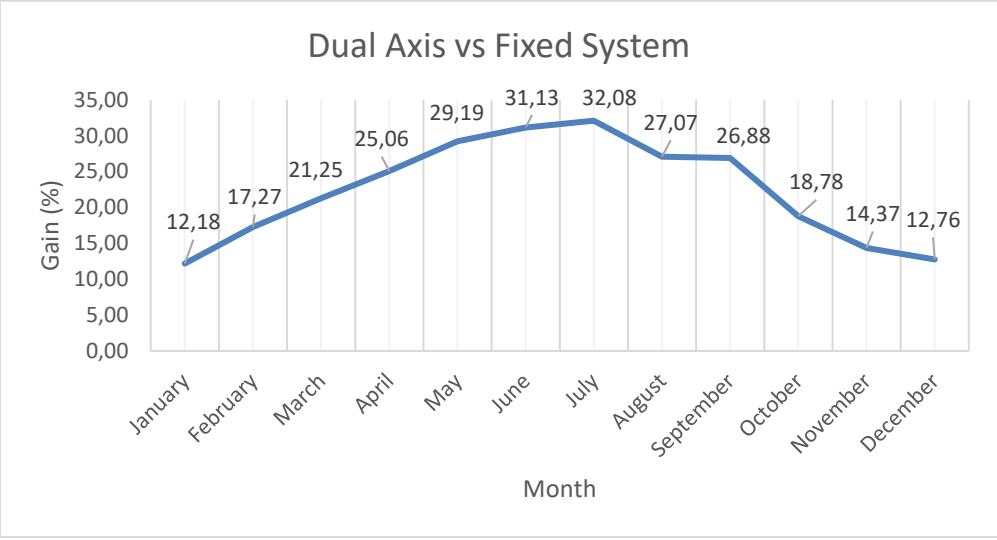

Figure 49. Gain of dual axis system compared to a fixed axis system on a monthly basis (Koussa, Haddadi, Saheb, Malek, & Hadji, 2012)

Other research papers that have propagated tracking systems, offer similar results. One found an increase of 56% power output, when implementing a three-position single axis tracking system (Huang & Sun, 2007). Another paper done in Syria found a 30% increase in supplied power to the grid from a tracking system (Dakkak & Babelli, 2012).

4.1.2 Dual Axis Compared to Single Axis Tracking System

As seen from previous figures tracking systems offer significant gains to non-tracking systems. However, the question arises of the difference in electrical output of single axis versus dual axis systems. A paper published in Energy Procedia aims to answer that question by comparing the effects of the moving mechanisms on flat PV panels. The researchers tested a total of seven systems, a two-axis system (TAST), two vertical single axis tracking (VAYOS; VASOS), two incline single rotating axis systems (IAYOS; IASOS), and two flat plate panels (FPYOS; FPSOS). The latter three have yearly and seasonal slope angle optimisation. The results include data from the entire year and several conclusions were made. The authors found that when considering various sky states the two-axis system's electricity production compared to the best performing single axis system (IASOS) did not exceed 5%. When taking into account the third best performing system (VASOS), the gain percentage remained low, not going over 7%. Figure 50 below shows a graphical representation of the data. (Koussa, Haddadi, Saheb, Malek, & Hadji, 2012)

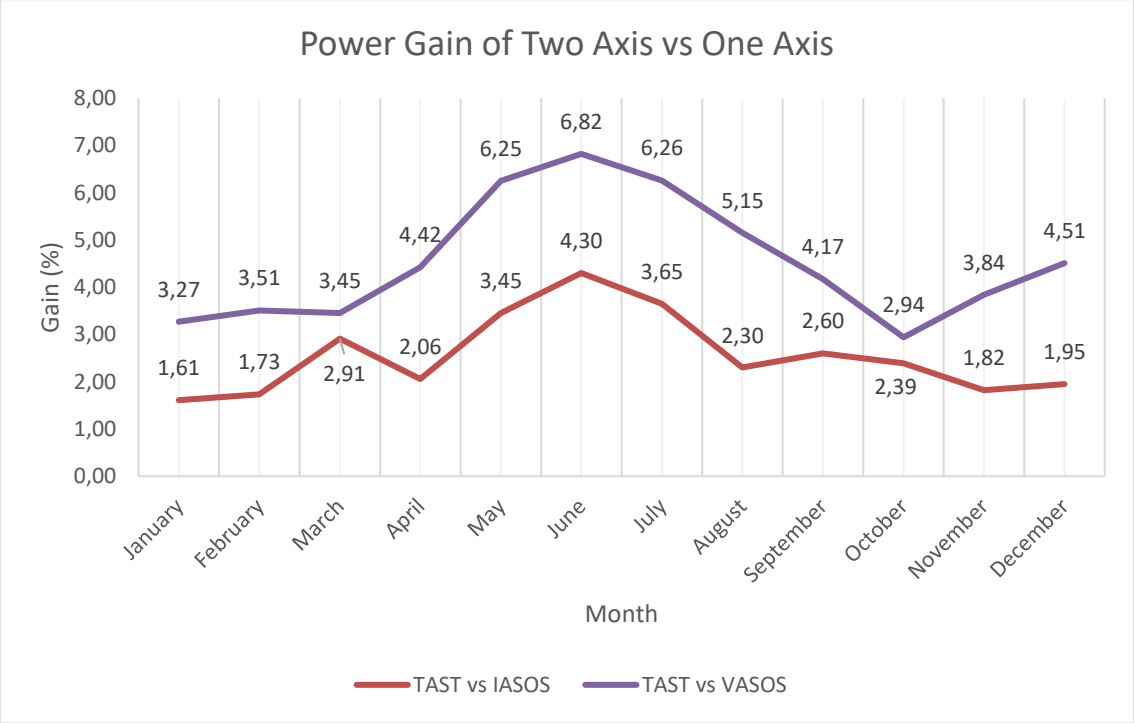

Figure 50. Power gain of a dual axis system as compared to two single axis systems. (Koussa, Haddadi, Saheb, Malek, & Hadji, 2012)

These results consider the systems with seasonal slope optimisation, when comparisons are drawn with yearly slope optimisation systems the results speak slightly more in favour of a two-axis systems, with the biggest recorded gain being just under 12%. The

study also calls into question the economic benefit of a two-axis system, as the extra investment costs cannot be rationalised by the minimal power gain. (Koussa, Haddadi, Saheb, Malek, & Hadji, 2012)

Admittedly, this data represents climate that is different from that of Finland's, in order to draw more geographically accurate assessment, a similar study must be conducted in regions where irradiation levels are comparable to those of Nordic states.

4.2 **Motor Programming Results**

The program showed mixed results. Testing shows that the single axis feature is in proper working condition and can realistically be set up for real-life tracking. This mode only requires one moving motor (Motor A), with the other one (Motor B) being set at 30°. Motor A's manual movement is reliable and simple for the end user. The normal day to day panel movement from east to west was also successful in its implementation. After the day is over the panel reverts back to the morning position in anticipation of the next sunrise. Occasionally, a tracking error originating from the Siemens Phi angle calculation function block will appear. When this occurs, the panel will automatically revert to the middle position, acting as a stationary panel until the issue is resolved. Success was also apparent in the "Timed Movement" feature. Here the motors would operate within a user-given time frame, for which the default setting is 45 seconds, and remain stationary for a set period of time as instructed. This stationary period is also adjusted by the user with the default setting being 20 minutes.

The dual axis mode however has shown uninspiring results. Whilst the tracking feature of this mode is in proper working condition, its control system has displayed an issue. Occasionally, when motor A moves, it will compromise the position feedback system of motor B; subsequently, the position of motor B will be read as inaccurate by the system and it will try to correct it. Often times, in the middle of this correcting movement the positional feedback system will revert to accurate readings which causes further erratic motor movement. The same effect is true when motor B is the initial moving motor. This error does not materialize in manual mode, when the motors are controlled by the user.

There are two factors that are suspected to be the cause of this fault:

- Both motors are connected to the same power supply.
- Usage of unreliable voltage regulators for the motor positional feedback system.

Problems started arising when the second motor was added to the system. Due to circumstances, there were hardware limitations imposed on the project, and further research in the troubleshooting of those issues did not fit the timetable of the thesis work. Dual axis tracking requires precise and efficient tracking for it to have value in terms of energy production and energy usage. The system's dual axis tracking feature is still present, and after some modifications it can be utilized as a research tool for the university. However, it is the authors' recommendation that in its current state, the single axis feature should be the focal point of study related utilization such as system functionality, energy measurements, and other data gathering.

4.3 **Upgrades and Recommendations**

There are a number of upgrades that can be added to the system to either increase serviceability, accuracy, or add new features. As stated before, this is a closed loop system. This means that it does not rely on a light sensor to dictate tracking, but rather an algorithm. Whilst algorithmic tracking is precise, a mixed open loop and closed loop system can provide a redundancy in the case of failure from the tracking system.

Other upgrades consider the system's serviceability. Implementing two separate power supplies for the motors might tackle a reoccurring issue with motor movement detailed in chapter 4.2. Additionally, the voltage regulators can be eliminated from the design if the motors' feedback system can be fed a stable 10VDC supply. This would eliminate inconsistencies that affect the motor position value in the program.

5 CONCLUSION

This thesis project aimed to explore the programming of linear motors in an attempt to create a solar tracking panel system, and to examine the value of sun tracking as opposed to fixed panels.

The program described in this paper utilizes Siemens' adaptation of a sun tracking algorithm to create single and dual axis tracking. The former proved to be a reliable method in a both constant tracking and timed movement mode. It uses a comparative function to determine the type of movement needed for the motor position to be at the desired sun angle, which is derived from the algorithm. Timed movement functions similarly, with the difference being the user-controlled wait time between the motor movement. This method can be generally used to minimize power consumption from the system. Results from the dual axis tracking feature were not as promising, with erratic motor movement occurring too often for the system to be reliable. However, with a number of corrective measures described earlier in the thesis, this issue could be mitigated, and a function dual axis mode could be attained.

Given the fact that Finland does not generally provide wide-spread support for solar energy through incentives and tax breaks, it is imperative that efficiency is increased in these systems in order for them to be competitive with other energy sources. Research showed that depending on the season, power gain from tracking panels as compared to stationary ones, was significant. This gain ranged from 12% during low irradiation months to over 50% during high irradiation months. Further analysis showed that dual axis systems do not provide any substantial benefit over single axis systems. The gain in this case, ranging from 1.6% to under 7% is the best-case scenario and did not account for the economic costs of establishing more complicated systems.

During the writing of this paper, access to the HAMK laboratory was severely limited, making it difficult for the authors to acquire new equipment as several obstacles became apparent. As a result of this, the implementation of hardware repairs was problematic.

In conclusion, despite setbacks, the system produced favourable results with only a few minor adjustments needed for full functionality. With the world constantly looking at renewables as an alternate, clean energy source, solutions which increase their efficiency will always be important and integral to society's energy needs.

References

Appunn, K., & Wehrmann, B. (2019, October 21). *Germany 2021: when fixed feed-in tariffs end, how will renewables fare?* Retrieved from Energy Post: https://energypost.eu/germany-2021-when-fixed-feed-in-tariffs-end-how-will-renewables-fare/

Chmielewski, T. (2017, April 25). *What Is Sun Transit & Moon Transit?* Retrieved from sciencing.com: https://sciencing.com/sun-transit-moon-transit-6559892.html

Dakkak, M., & Babelli, A. (2012). Design and Performance Study of a PV Tracking System (100W-24Vdc/220Vac). *Energy Procedia, 19*, 91-95. Retrieved from http://www.sciencedirect.com/science/article/pii/S1876610212009587

Eke, R., & Senturk, A. (2012). Performance comparison of a double-axis sun tracking versus fixed PV system. *Solar Energy, 86*(9), 2665-2672. Retrieved from http://www.sciencedirect.com/science/article/pii/S0038092X12002174

Eldin, S. S., Abd-Elhady, M., & Kandi, H. (2016). Feasibility of solar tracking systems for PV panels in hot and cold regions. *Renewable Energy, 85*, 228-233. Retrieved from http://www.sciencedirect.com/science/article/pii/S0960148115300744

European Commission. (2020). *Europe 2020 targets: statistics and indicators for Finland.* Retrieved from European Commission: https://ec.europa.eu/energy/sites/ener/files/documents/necp_factsheet_fi_final.pdf

Finnish Institution for Health and Welfare. (2020). Situation update on coronavirus. Helsinki, Finland. Retrieved from https://thl.fi/en/web/infectious-diseases/what-s-new/coronavirus-covid-19-latest-updates/situation-update-on-coronavirus

Hakkarainen, T., Tsupari, E., Hakkarainen, E., & Ikäheimo, J. (2015). *The role and opportunities for solar energy in Finland and Europe.* Espoo: VTT Technical Research Centre of Finland Ltd.

Huang, B., & Sun, F. (2007). Feasibility study of one axis three positions tracking solar PV with low concentration ratio reflector. *Energy Conversion and Management, 48*(4), 1273-1280. Retrieved from http://www.sciencedirect.com/science/article/pii/S0196890406003050

Koussa, M., Haddadi, M., Saheb, D., Malek, A., & Hadji, S. (2012). Sun Tracking Mechanism Effects on Flat Plate Photovoltaic System Performances for Different Step Time and Main Parameters Affecting the Obtained Gains: Case of North Africa and Mediterranean Site. *Energy Procedia, 18*, 817-838. doi:10.1016/j.egypro

Morrison, L. V., & Stephenson, F. R. (2004). Historical values of the Earth's clock error ΔT and the calculation of eclipses. *Journal for the History of Astronomy, 35*(3), 327 - 336. Retrieved from http://articles.adsabs.harvard.edu//full/2004JHA....35..327M/0000327.000.html

Official Statistics of Finland. (2019). *Energy supply and consumption.* Ministry of Finance. Helsinki: Statistics Finland. Retrieved 2020, from http://www.stat.fi/til/ehk/index_en.html

Official Statistics of Finland. (2019). *Production of electricity and heat.* Ministry of Finance. Helsinki: Statistics Finland. Retrieved 2020, from http://www.stat.fi/til/salatuo/index_en.html

Prinsloo, G., & Dobson, R. (2015). *Solar Tracking.* SolarBooks. doi:10.13140/2.1.2748.3201

Reca-Cardeña, J., & López-Luque, R. (2018). Chapter 9 - Design Principles of Photovoltaic Irrigation Systems. In J. Reca-Cardeña, R. López-Luque, & I. Yahyaoui (Ed.), *Advances in Renewable Energies and Power Technologies: Volume 1: Solar and Wind Energies* (pp. 295-333). Elsevier Science.

Reda, I., & Andreas, A. (2008). *Solar Position Algorithm for Solar Radiation Applications.* United States Government, U.S. Department of Energy. National Renewable Energy Laboratory. Retrieved from https://www.nrel.gov/docs/fy08osti/34302.pdf

RS Components Ltd. (n.d.). *Datasheet: RS PRO.* Retrieved 2020, from RS Components Ltd: https://docs.rs-online.com/7cd8/0900766b8168345e.pdf

RS Components Ltd. (n.d.). *RS PRO Electric Linear Actuator, 24V dc, 300mm stroke.* Retrieved 2020, from RS Components: https://uk.rs-online.com/web/p/linear-actuators/1774513/

Siemens. (2016, September 16). *SIMATIC S7 S7-1200 Programmable controller.* Retrieved from Siemens Industry Online Support: https://support.industry.siemens.com/cs/document/109741593/simatic-s7-s7-1200-programmable-controller?dti=0&lc=en-WW

Siemens. (2018, 10 26). *Delivery Release SIMATIC STEP 7 Professional / Basic V15.1*. Retrieved from Siemens Industry Online Support: https://support.industry.siemens.com/cs/document/109758795/delivery-release-simatic-step-7-professional-basic-v15-1?dti=0&lc=en-US

Siemens. (2019, January). *Product Support.* Retrieved from Industry Online Support.

Siemens AG. (2010). *Compact Switch Module Siemens CSM 1277 - 6GK7277-1AA10-0AA0.* Retrieved from Automation24:

https://media.automation24.com/manual/en/36087313_BA_S7-1200-CSM1277.pdf

Siemens AG. (2020, January). *Calculation of Alignment for Single-Axis Solar Tracker.* Retrieved from Solar Tracking with S7-1200 / S7-1500: https://support.industry.siemens.com/cs/document/109775729/solar-tracking-with-s7-1200-s7-1500?dti=0&lc=en-WW

Siemens AG. (2020, January). *Solar Position Algorithm (SPA).* Retrieved from Solar Tracking with S7-1200 / S7-1500: https://cache.industry.siemens.com/dl/files/729/109775729/att_1012177/v2/109775729_SOLAR_SPA_DOC_V10.pdf

Tang, Y.-w. (2014, January 1). Effects of parameters on NREL Solar Position Algorithm (SPA) and SIMATIC S7-1200 SPA_Calc_SunVector library accuracy. *Journal of Applied Engineering Technology, 2*(1), 133-150. doi: 10.7112/JAET